

C. 183

NASALOAN COPY: RETURN
AFWL (WLL—)
KIRTLAND AFB, N.

0063040

**MEMORANDUM**

EXPERIMENTALLY DETERMINED EFFECTS OF VARYING PITCH AND
CONTROL STIFFNESSES ON THE FLUTTER CHARACTERISTICS AT
SUPERSONIC SPEEDS OF ALL-MOVABLE
WING AND TAIL MODELS

By Perry W. Hanson

Langley Research Center
Langley Field, Va.

This material contains information affecting the National Defense of the United States within the meaning
of the espionage laws, Title 18, U.S.C., Sec. 793 and 794, and the transmission or the revelation of its
contents in any manner to an unauthorized person is prohibited by law.

**NATIONAL AERONAUTICS AND
SPACE ADMINISTRATION**WASHINGTON
March 1959

1183

Classification canceled (or changed to _____)

by authority of NASA Classification Change Notice #170- dtl 7/20/66 by _____

authorizing change

Linda Beattie - GS 2 12 September 1966

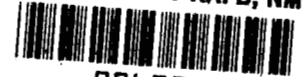
Name & Grade of Officer making change

Date

2 cds removed 21 Jan 64 fr

[REDACTED]
NATIONAL AERONAUTICS AND SPACE ADMINISTRATION

TECH LIBRARY KAFB, NM



0063040

MEMORANDUM 10-16-58L

EXPERIMENTALLY DETERMINED EFFECTS OF VARYING PITCH AND
CONTROL STIFFNESSES ON THE FLUTTER CHARACTERISTICS AT
SUPERSONIC SPEEDS OF ALL-MOVABLE

WING AND TAIL MODELS*

By Perry W. Hanson

SUMMARY

The flutter characteristics of geometrically, dynamically, and elastically scaled variable-incidence wing, all-movable horizontal-tail, and vertical-tail models of a proposed fighter airplane were investigated in the Langley 9- by 18-inch supersonic flutter tunnel at Mach numbers of 1.3, 1.64, 2.0, and 2.55. The effects of varying the aileron and rudder control stiffnesses and pitch stiffness were also investigated. A proposed method of compensating for an all-movable flutter-model mounting system having an inertia greater than the scaled value was evaluated and was found to be satisfactory. The specific models with scaled design pitch stiffnesses and control stiffnesses proved to be free from flutter within the required scaled flight boundary. Except for extremely low values of pitch stiffness, the dynamic pressure at flutter varied almost linearly with the pitch stiffness of the wing models tested. The numerical value of the dynamic pressure at flutter was more sensitive to changes in pitch stiffness with increasing Mach number although the percent change in flutter dynamic pressure was nearly constant up to a Mach number of 2.0.

INTRODUCTION

The increased usage of highly swept all-movable surfaces for stabilization and control of airplanes and missiles coupled with the frequent occurrence of flutter of these surfaces has led to considerable interest in a study of their flutter characteristics. At the present time analytical methods for the prediction of the flutter behavior of such

*Title, Unclassified.
[REDACTED]


1183

surfaces are useful primarily for trend studies and their use as criteria for design is questionable. Although some experimental trend studies have been made (see, for instance, refs. 1 to 4), they are for the most part limited in scope since they use scaled models of proposed controls. The designer, therefore, is presently faced with the problem of having to determine experimentally the flutter characteristics of each particular configuration he may wish to use. Thus, a flutter investigation involving both specific and general research of geometrically, elastically, and dynamically scaled models of the variable-incidence wing, all-movable horizontal tail, and of the vertical tail of a proposed fighter airplane has been made in the Langley 9- by 18-inch supersonic flutter tunnel for the Mach number range from 1.3 to 2.55. The wing and vertical tail were tested with and without controls. All models were wall-mounted and tested separately. The purpose of the investigation was threefold: To determine whether the models were flutter-free within the scaled required flight boundary; to investigate the effects of changing the wing and horizontal-tail pitch stiffnesses and the aileron and rudder control stiffnesses; and to evaluate a proposed method of compensating for an all-movable control model having a mount-assembly inertia greater than the scaled value. The investigation, accordingly, is presented in three phases which parallel these areas of interest.

SYMBOLS

a	speed of sound, fps
e	distance from control center of gravity (aileron or rudder) to hinge line, in.
f_f	flutter frequency, cps
f_n	natural vibration frequency of nth mode ($n = 1, 2, 3, 4, 5$), cps
I_c	mass moment of inertia of control surface about control hinge line, in-lb-sec ²
I_f	mass moment of inertia of model mounting flange about pitch axis, in-lb-sec ²
I_m	mass moment of inertia of basic-model mount assembly about pitch axis, in-lb-sec ²

I_O	mass moment of inertia of modified mount assembly about pitch axis (or for purposes of developing equation (A2), the mount assembly pitching inertia not representative of scaled value of airplane-wing center-bay inertia), in-lb-sec ²
I_p	mass moment of inertia about pitch axis of model exposed panel (excluding mounting flange and instrumentation wire), in-lb-sec ²
I_t	mass moment of inertia of model including mounting flange and with instrumentation wire about pitch axis, in-lb-sec ²
K	wing and horizontal-tail pitch stiffness, in-lb/radian
K_c	aileron or rudder control effective hinge stiffness, in-lb/radian
K_O	pitching stiffness required for model wing with increased (unrepresentative) mount assembly inertia to give correct impedance at flutter frequency based on relation $K_O = K + 4\pi^2 f_f^2 (I_O - I_m), \text{ in-lb/radian}$
l	distance from model root to panel center of gravity measured perpendicular to model root, in.
M	Mach number
q	dynamic pressure, lb/sq ft
q_f	dynamic pressure at flutter for basic mount-model configuration, lb/sq ft
$q_{f,0}$	dynamic pressure at flutter for model with pitch stiffness changed to compensate for an increased (unrepresentative) mount assembly inertia, lb/sq ft
r	distance from pitch axis to panel center of gravity measured parallel to root chord (positive when center of gravity is forward of pitch axis), in.
R_f	correct impedance of model mount assembly at flutter frequency, in-lb/radian
W_c	weight of control surface, lb
W_m	weight of moving portion of basic-wing mount assemblies and horizontal mount assemblies, lb



W_0	weight of moving portion of modified-wing mount assemblies, lb
W_f	weight of wing and horizontal-tail mounting flanges, lb
W_p	weight of model panel excluding mounting flange and instrumentation wire, lb
W_t	total weight of wing including flange and instrumentation wire, lb
W_w	weight of instrumentation wire, lb
ρ	test-section density, slugs/cu ft


APPARATUS AND OPERATING PROCEDURE

Wind Tunnel

This investigation was made in the Langley 9- by 18-inch supersonic flutter tunnel which is a conventional, fixed-nozzle, blowdown wind tunnel exhausting into a vacuum sphere from a pressure reservoir. The nozzle configurations used gave Mach numbers of 1.3, 1.64, 2.0, and 2.55. At each Mach number the test-section density varies continuously to a controlled maximum density and then decreases. Maximum test-section conditions are depicted in the tunnel performance curves shown in figure 1.

The test procedure for all Mach numbers was essentially the same. The test section and the sphere into which the tunnel exhausts, were pumped down to a pressure of approximately 2 pounds per square inch absolute. The control valve upstream of the test section was then opened and the test-section density was allowed to increase until flutter was observed or the maximum density obtainable was reached. After each run the models were inspected visually and the natural frequencies were checked and compared with those obtained just prior to the run to determine whether any structural changes had occurred.

The models were mounted on the mount blocks through the mount assembly. The mount blocks, in turn, were attached to the head of a ram that was used to inject or retract the models through one side of the test section in order to avoid rough flow during the starting and stopping operation. The models were viewed through a window in the opposite side of the test section.



The actual time for each run was approximately 3 to 4 seconds. A multichannel oscillograph provided a continuous record of the test conditions and of the behavior of resistance wire strain-gage bridges attached to the model box spars. A 16-millimeter motion-picture camera, operated at approximately 1,000 frames per second, furnished a record of the model motions.

Models

This investigation employed geometrically, elastically, and dynamically scaled surfaces of the variable-incidence wing, the all-movable horizontal tail, and the vertical tail of a fighter-type airplane. However, the wing and horizontal-tail mount assemblies (that portion of the mount-model combination corresponding to the center bay of the airplane fuselage-wing combination) were not dynamically scaled. The basic wing models are designated W1 to W6, the first two of the series being without ailerons. Three of the wing models (W2, W5, and W6) were repaired and redesignated W2A, W5A, and W6A for use in the third phase of the investigation. The wing mount was strengthened for the third phase of the investigation; this strengthening resulted in an increase in weight and a slight increase in inertia. When these latter three wings were tested in combination with various mount inertias, the configurations are identified by suffixing the numbers 1 to 4 to the three redesignated models. (These configurations are defined in table V.)

The all-movable horizontal-tail models are designated HT-1, HT-4, and HT-5 and the vertical tail models, VT-3, VT-4, and VT-7. Vertical tail models VT-3 and VT-4 had hinged (leaf spring) rudders.

Model Geometry

The wing models were 0.0333 scale and had an exposed panel aspect ratio of 1.71 and a taper ratio of 0.246 based on a tip chord not including the leading-edge extension. The geometry of the wing models is shown in figure 2(a).

The horizontal-tail models were 0.0662 scale and had an exposed panel aspect ratio of 1.59 and a taper ratio of 0.196. The geometry of the horizontal-tail models is shown in figure 2(b).

Both the wing and the horizontal-tail models were effectively all-movable surfaces. The wing pitch axis was at 69.4 percent of the root chord and the horizontal-tail pitch axis was at 51.4 percent of the root chord.

The geometry of the vertical tail is shown in figure 2(c). The vertical-tail model was 0.065 scale and had an aspect ratio of 1.20 and a taper ratio of 0.359. Unlike the wing and horizontal tail, the vertical tail was not free to pitch. The bending moment was taken by a

1/2-inch-square aluminum mount rod located at 69.2 percent of the root chord, the model being restrained in the pitching degree of freedom by two shear bolts at 25 percent of the root chord. The vertical tails normally carried a concentrated mass representing tail warning radar on the trailing edge at 75.7 percent span.

Construction

All the models were constructed in the same general manner. The details of construction of the various models are shown in figure 3. The main load carrying member of each model was a tapered hollow aluminum box spar to which aluminum-alloy ribs were welded. Spruce or mahogany leading and trailing edges were glued to the ends of the ribs to complete the plan form. Mounting flanges were welded to the roots of the box spars except for the vertical-tail models which had a 1/2-inch-square aluminum mounting bar extending into the box spar. Electrical resistance wire strain gages were mounted on the box spars near the root. Balsa wood was used to fill in the area between the structural members and to give the models their airfoil shapes. Pieces of lead were used to obtain desired mass and inertia distribution. The balsa was then covered with model silk and doped. The aileron and rudder controls were similarly constructed. The frames consisted of spruce leading and trailing edges connected in the streamwise direction by aluminum-alloy ribs two of which carried hinge mounts on the upstream ends.

Model Mounting Systems

The mount assemblies of all the models were built into aluminum mounting blocks (approximately 1.5 by 2.8 by 12 inches) which were attached to the head of the tunnel injector mechanism. A drawing of the wing mount assembly is shown in figure 4(a). The assembly consisted of a flange mount (to receive the model flange) welded to the main mount-assembly member, the downstream end of which was attached to a leaf spring secured to the mounting block. The upstream end was attached to an auxiliary spring which was in turn attached to the mounting block by a bolt that could be moved in the chordwise direction. Thus, the pitch stiffness of the wing mount assembly could be changed by moving this bolt to change the effective length of the auxiliary spring, and/or by using springs of different thicknesses. The mount assembly, except for the area around the flange mount, was enclosed by a cover plate.

The horizontal-tail mount assembly was similar to the wing mount assembly except that no auxiliary spring was used. Figure 4(b) shows the details of this mount. The flange mount that received the horizontal-tail flange was cantilevered on a leaf spring secured to the mounting

block. The pitching stiffness was changed by using leaf springs of various thicknesses.

The vertical-tail mount assembly consisted simply of a hole in the mounting block to receive the square aluminum mounting bar with set screws through the block to secure the bar. Two holes were tapped in the upstream face of the block to receive the shear bolts on the model root. (See fig. 2(c).)

Physical Properties

The physical properties of the basic model configurations are given in table I and the physical properties of the modified wing-mount configurations are given in table II. Table III(a) presents typical weight and inertia distribution of the model wings without ailerons. The geometric boundaries of the various stations along with the centers of gravity are presented in figure 5(a). Typical weight and inertia distributions of wing models with ailerons are shown in table III(b) and the boundaries of the various stations and the centers of gravity are shown in figure 5(b). Table III(c) gives a typical weight and inertia distribution of models of the horizontal tail. Figure 5(c) defines the boundaries of the stations and the centers of gravity.

Representative mode shapes of the first three natural modes of vibration of a wing without aileron for two different pitch stiffnesses are presented in table IV. The models were excited by an acoustical shaker and the mode shapes determined by the acceleration method described in reference 5. Typical node lines for various pitch stiffnesses and control hinge stiffnesses of some of the various models tested are presented in figure 6. Pitch stiffnesses were measured by an optical lever method, the estimated maximum error of which varied from approximately 2 percent at a pitch stiffness of approximately 4,000 inch-pounds per radian to 5 percent at 18,000 inch-pounds per radian. Varying the wing pitch stiffness over a wide range generally produced little change in the frequencies and node lines. The first and second natural vibration modes were more sensitive to pitch stiffness variations than the higher modes. As the pitch stiffness was increased over a wide range, the first-mode frequency increased slightly and the node line moved somewhat closer to the root. The second-mode frequency also increased slightly and the node line near the root moved toward the tip slightly while the node line near the tip displayed no apparent change.

Changing the aileron or rudder hinge stiffness over a wide range produced considerable change in the node lines of the higher modes on both the wing and vertical-tail models. Reducing the pitch stiffness of the horizontal-tail models by one-half lowered all the natural frequencies but had little effect on the node lines except for the fifth

mode. The fifth-mode natural frequency was somewhat insensitive to pitch stiffness changes, but the node line changed considerably.

TEST PROGRAM

The test program was divided into three phases. The purpose of the first phase was to determine whether the wing and horizontal-tail models with the scaled design pitch stiffnesses and the vertical-tail models with the scaled design bending stiffness were free from flutter within the predicted flight boundary of the airplane (including the required safety margin). During this phase of testing, the aileron and rudder hinge stiffnesses were reduced below the scaled design values to determine the effect on the wing and horizontal-tail flutter boundary. The second phase of the test program was to determine the effect of varying the pitch stiffness of the basic wing-mount configuration at the various Mach numbers tested. The third phase was concerned with an experimental assessment of an analytical method proposed in reference 6 for compensating for unrealistic mount assembly inertias. It was mentioned in the section on models that the center-bay or mount assembly of the wing model was not dynamically scaled. It was not practical to build the mount assembly with as little mass as the scale factor indicated; as a result the mount assembly was too massive. The proposed method for compensating for this condition is developed in the appendix.

The models used in the third phase of the investigation were three reworked models and the mount assembly was salvaged from the first phase. The models (W2A, W5A, and W6A) and mount assemblies used in this phase are referred to as "modified" in that the mass of the mount assembly was increased to various values over that of the mount assembly as originally designed. The test procedure used in this phase was as follows: A model with the mount-assembly inertia approximately as originally designed and with a certain pitch stiffness was run in the tunnel to determine the flutter frequency and the dynamic pressure at flutter. The inertia of the mount assembly was then changed and the pitch stiffness altered according to the relation developed in the appendix: $K_0 = K + 4\pi^2 f_f^2 (I_0 - I_m)$. The model was again tested to determine whether the dynamic pressure at flutter remained the same, in order to verify the effectiveness of the compensation. This was done for several pitch stiffnesses K at $M = 1.30$ and 1.64 . In addition, the pitch stiffness K was held constant and the mount-assembly inertia was changed by various amounts; the pitch stiffness necessary to compensate for these various increased inertias was then calculated and the models were tested with the new pitch stiffness and inertia. It should be mentioned that the pitch stiffnesses at which the models were actually tested generally were not exactly the calculated value of K_0 .

because of the practical factors involved in setting the pitch stiffnesses precisely. The difference between the calculated values of K_0 and the measured values are shown in table V which also presents a summary of the weight, inertia, and pitch-stiffness variations for the wing model configurations used in the third phase of the investigation.

RESULTS AND DISCUSSION

First Phase

The wing, horizontal-tail, and vertical-tail experimental results of the first phase of the investigation are presented in table VI(a). Wing models were run at $M = 1.3, 1.64, 2.0, \text{ and } 2.55$ with the pitch stiffness and aileron stiffness set at approximately the scaled design value without any flutter being encountered within the scaled flight boundary with the required safety margin.

The aileron stiffness of the various models was progressively reduced in order to determine the effect on the wing flutter characteristics. Aileron flutter at 400 cycles per second was encountered at $M = 1.3$ when the aileron stiffness of model W5 was set at approximately one-tenth the scaled design value. Motion pictures of the test indicated that the oscillation was a pure flapping motion about the aileron hinge line.

Horizontal-tail models with a pitch stiffness approximately equal to the scaled design value were tested at $M = 1.3, 1.64, 2.0, \text{ and } 2.55$ without encountering flutter within the scaled flight boundary including the safety margin. In order to define the stiffness safety margin, the pitch stiffness was reduced until constant-amplitude flutter at 300 cycles per second was encountered with model HT-5 at a dynamic pressure of 3,225 pounds per square feet at $M = 1.30$. The pitch stiffness was approximately 60 percent of the scaled design value. When the pitch stiffness of model HT-5 was reduced to approximately 50 percent of the scaled design value, destructive flutter was encountered at a dynamic pressure of 2,940 pounds per square foot at $M = 1.3$. A confirmation test was made with model HT-4 with a pitch stiffness of approximately 60 percent of the scaled design value. The model fluttered at a dynamic pressure of 2,940 pounds per square foot at $M = 1.3$. The flutter modes for both the wing and horizontal tail appeared to be a strong coupling at the second bending mode and pitching mode.

It may be noted that the inertias of both the wing and horizontal-tail mounts were greater than the scaled design values. As will be shown in the discussion of the third phase of the investigation, increasing the

mount inertias caused a decrease in the flutter dynamic pressure; therefore, the test results of this phase may be considered to be conservative. Vertical-tail model VT-4 was tested at $M = 1.3, 1.64, 2.0,$ and 2.55 at approximately the scaled design rolling stiffness and rudder stiffness without encountering flutter within the limits of the tunnel, although a region of low damping was encountered at a dynamic pressure of 2,540 pounds per square foot at $M = 1.3$ and 2,725 pounds per square foot at $M = 1.64$. However, the model did not flutter. A maximum dynamic pressure of approximately 3,370 pounds per square foot at $M = 1.3$ and 3,760 pounds per square foot at $M = 1.64$ and above simulated the required flight boundary. The rudder stiffness was then progressively reduced at $M = 1.3$ to approximately 40 percent of the scaled design value without encountering flutter, although regions of low damping were encountered as before. Runs 102 and 104 were made to determine the effect of removing the mass that simulated the tail warning radar. No effect was evident.

Second Phase

The second phase of the investigation was concerned with determining the effect of large changes in wing model pitch stiffnesses on flutter at the various Mach numbers. The experimental results are presented in table VII and in figure 7 which shows the variation of dynamic pressure at flutter with pitch stiffness for several Mach numbers. Although the range of pitch stiffnesses covered is rather wide, little change was evident in the natural frequencies and node lines, and the wing models appeared to flutter in the same mode regardless of pitch stiffness except for the very low pitch stiffness of 460 inch-pounds per radian. The typical flutter mode appeared to be a strong coupling of a pitch mode and the second bending mode. The flutter mode for a pitch stiffness of 460 inch-pounds per radian appeared to start as a pure pitching motion that slipped into the typical flutter mode almost immediately. Figure 8 shows frames taken from a high-speed 16 millimeter motion picture which illustrate the typical wing flutter mode. From figure 7 it can be seen that, except for very low pitch stiffnesses, the dynamic pressure at flutter varied almost linearly with the pitch stiffness. The effect of a given change in pitch stiffness on the numerical value of the flutter dynamic pressure appears to become more pronounced with increasing Mach number, although the percent change was approximately the same for Mach numbers up to 2.0.

Third Phase

The third phase of the investigation was an experimental assessment of a proposed method (presented in the appendix) of compensating for a scaled model mounting system having a mass and inertia greater than the

scaled value, which is very often the case in scaling all-movable model mounts. In the present investigation, a model was fluttered with a certain mounting system inertia I_m and pitch stiffness K which were assumed to represent the correctly scaled values of a hypothetical prototype. The inertia of the mounting system was then increased. In order to compensate for this increased ("incorrectly scaled") inertia I_0 , the pitch stiffness K was increased to K_0 according to the relation $K_0 = K + 4\pi^2 f_f^2 (I_0 - I_m)$ where f_f is the flutter frequency of the model with a "correctly scaled" mount inertia. This model was then fluttered and the flutter frequency and dynamic pressure were compared with those of the first model configuration. This was done for several values of pitch stiffness K and the corresponding flutter frequencies f_f while the amount of increase in inertia $I_0 - I_m$ remained the same. If application of the method compensates exactly for the increased inertia, the dynamic pressure at flutter for the two configurations would be the same. The experimental results of this phase of the investigation are presented in table VIII. In figure 9(a), the ratio of the dynamic pressure at flutter for the model with the pitch stiffness changed to compensate for an increased (approximately 2.3 times), unrepresentative mount-assembly inertia to the dynamic pressure at flutter for the basic mount-model configuration is plotted against the basic pitch stiffness. (The numbers beside the data points indicate the runs from which the ratios were determined.) For the basic pitch stiffness range investigated, increasing the pitch stiffness according to the relation $K_0 = K + 4\pi^2 f_f^2 (I_0 - I_m)$ to compensate for the increased mount inertia generally held the dynamic pressure at flutter for the increased-mount-inertia configuration to within 10 percent of the flutter dynamic pressure except for one run for the basic configuration.

Generally, the method overcompensated slightly since the dynamic pressure at flutter for the increased-mount-inertia configuration was greater than that for the basic configuration. For comparison, one model with increased mount inertia was fluttered without compensating for the increased stiffness with the result that the model fluttered at a dynamic pressure of about 45 percent less than that for the basic model configuration. On run 122, the model with increased mount inertia fluttered at a dynamic pressure 25 percent greater than that for the basic configuration. This excessive overcompensation may have been due to an error in setting the pitch spring. A similar model, fluttered under the same comparative conditions, showed only a 5 percent increase in flutter dynamic pressure.

Since the proposed method of compensating for too great a mount inertia appeared to be satisfactory over a range of pitching stiffness for an increase in inertia at approximately 2.3 times that of the basic

configuration, the method was next checked for applicability at other mount inertia increments but for only one basic configuration pitch stiffness of approximately 6,000 inch-pounds per radian. The results are shown in figure 9(b). The mount inertia was increased from 1.6 to 2.9 times the basic mount inertia and was compensated for by increasing the pitch stiffness according to the proposed method. Again application of the method appeared to overcompensate slightly. The flutter dynamic pressure for the increased-mount-inertia configurations averaged about 10 percent higher than the flutter dynamic pressure for the basic configuration, with a maximum increase in flutter dynamic pressure of approximately 20 percent. Again, for comparison, the mount inertia was increased 2.9 times for one run without compensating for the increased inertia. This configuration fluttered at a dynamic pressure about 50 percent less than that for the basic mount inertia. When the pitch stiffness was changed to compensate for the increased mount inertia, the flutter dynamic pressure was 7 percent greater than that for the basic mount configuration.

In this phase of the investigation the flutter frequencies of the increased-mount-inertia configurations (when compensated for) were generally within 3 percent of those of the basic configurations; thus, the results added further confirmation to the validity of the method.

CONCLUSIONS

From the results of flutter tests of the variable incidence wing and all-movable horizontal-tail and vertical-tail models of a proposed fighter airplane, the following conclusions are made:

1. The wing models both with and without aileron, when flown at the scaled design pitch stiffness and control stiffness, were found to be free from flutter within the scaled predicted flight boundary (including the required safety margin) for the Mach numbers tested. The horizontal and vertical tails when flown at scaled design stiffnesses were also found to be free from flutter within the required scaled flight boundary.
2. The dynamic pressure required to flutter the all-movable wings at reduced pitch stiffness varied almost linearly with pitch stiffness except for extremely low values.
3. The numerical value of the dynamic pressure at flutter was more sensitive to changes in pitch stiffness with increasing Mach number although the percent change in dynamic pressure was nearly constant up to a Mach number of 2.0.

4. A proposed method for compensating for an all-movable model mount having an inertia greater than the scaled design value appears to have merit within the range of pitch stiffness and excess inertia investigated.

Langley Research Center,
National Aeronautics and Space Administration,
Langley Field, Va., August 15, 1958.

APPENDIX

**A METHOD OF COMPENSATING FOR EXCESSIVE INERTIA
IN THE ROOT REGION OF FLUTTER MODELS**

Generally the exposed surface of a flutter model can be fairly accurately scaled geometrically, elastically, and dynamically. However, in all-movable models the spring systems used to simulate the scaled pitching restraint often are not consistent with the scaled inertial properties of the airplane all-movable control actuating system. Also, the size of the model mount system is frequently determined by the facility in which the model is being tested. Thus the inertial properties of the root region of flutter models may not be representative of the surface being scaled.

A method of compensating for the too massive root region by altering the scaled design pitching stiffness has been proposed by Mr. A. L. Head. This method may be developed in the following manner:

At the flutter frequency, if the impedance presented to the exposed surface by the root region is the same as the impedance which would be presented by the correctly scaled root region, it might be supposed that the model would have nearly the correct flutter characteristics. Consider the impedance presented to the exposed surface at flutter to be a combination of resistance to motion due to the mount-assembly inertia at the flutter frequency and resistance to motion due to the pitch spring. Then an undamped-mount-assembly impedance equation may be written as:

$$-I_m f_f^2 (2\pi)^2 + K = R_f = -I_0 f_f^2 (2\pi)^2 + K_0 \quad (A1)$$

or

$$K_0 = K + 4\pi^2 f_f^2 (I_0 - I_m) \quad (A2)$$

where

f_f flutter frequency, cps

I_m correctly scaled pitching mass moment of inertia, in-lb-sec²

K correctly scaled pitching stiffness, in-lb/radian

- R_f correct impedance of model mount assembly at flutter frequency,
in-lb/radian
- I_0 pitching mass moment of inertia of configuration that does not
have a representative root region, in-lb-sec²
- K_0 pitching stiffness required for configuration with unrepresentative
root region to give correct impedance at flutter
frequency, in-lb/radian

REFERENCES

1. Asher, Gifford W., Martuccelli, John R., and Weatherill, Warren H.: Flutter Model Tests of a Swept-Back, All-Moving Horizontal Tail at Supersonic Speeds. WADC Tech. Rep. 56-285. ASTIA Doc. No. AD-142088, U.S. Air Force, Nov. 1957.
2. Boswinkle, Robert W., Jr., and Morgan, Homer G.: Flutter Experiments With Various Control Configurations. NACA RM L57D23c, 1957.
3. Land, Norman S., and Abbott, Frank T., Jr.: Transonic Flutter Investigation of an All-Movable Horizontal Tail for a Fighter Airplane. NACA RM L56G06, 1957.
4. Morgan, Homer G., Figge, Irving E., and Presnell, John G., Jr.: Investigation of Flutter Characteristics of Three Low-Aspect-Ratio All-Movable Half-Span Control Surfaces at Mach Numbers From 1.49 to 2.87. NACA RM L58B20, 1958.
5. Hanson, Perry W., and Tuovila, W. J.: Experimentally Determined Natural Vibration Modes of Some Cantilever-Wing Flutter Models by Using an Acceleration Method. NACA TN 4010, 1957.
6. Head, A. L., Jr., and Morosow, G.: F8U-3 Airplane Flutter Model Test Results - Interim Report for Phase I Tests. Rep. No. 10675 (Contract NOa(s) 57-296), Chance Vought Aircraft, Inc. (Dallas, Texas), Dec. 16, 1957.

TABLE I.- PHYSICAL CHARACTERISTICS OF BASIC-WING, HORIZONTAL-TAIL, AND VERTICAL-TAIL MODELS

Model	W _p , lb	W _f , lb	W _w , lb	W _t , lb	W _m , lb	r, in.	l, in.	I _p , in-lb-sec ²	I _f , in-lb-sec ²	I _t , in-lb-sec ²	I _m , in-lb-sec ²	W _c , lb (*)	I _c , in-lb-sec ² (*)	e, in. (*)	Cantilevered frequencies (**)			
															f ₁ , cps	f ₂ , cps	f ₃ , cps	f ₄ , cps
W1	0.1002	0.0228	0.0039	0.1269	0.1287	-0.23	1.70	83.7 × 10 ⁻⁵	29.53 × 10 ⁻⁵	113.2 × 10 ⁻⁵	97.4 × 10 ⁻⁵	-----	-----	----	157	440	665	910
W2	.1041	.0228	.0039	.1308	.1287	-.16	1.92	74.1	29.53	103.6	97.4	-----	-----	----	157	438	662	940
W3	.1203	.0239	.0039	.1480	.1287	-.12	2.13	90.8	25.10	116.0	97.4	0.0074	0.363 × 10 ⁻⁵	0.30	137	382	605	836
W4	.1292	.0239	.0039	.1570	.1287	.09	1.92	91.7	25.10	116.8	97.4	.0074	.440	.29	146	395	636	880
W5	.1128	.0239	.0039	.1396	.1287	.04	1.98	90.4	25.10	115.5	97.4	.0077	.440	.34	142	400	632	870
W6	.1132	.0239	.0039	.1410	.1287	.03	1.95	104.4	25.10	129.5	97.4	.0072	.311	.28	147	410	642	855
HT1	.0907	.0182	.0035	.1124	.0163	.90	1.55	82.9	1.04	83.9	4.15	-----	-----	----	165	519	880	1,100
HT4	.0826	.0182	.0035	.1043	.0163	.92	1.50	88.1	1.04	89.1	4.15	-----	-----	----	170	530	900	1,055
HT5	.0933	.0182	.0035	.1150	.0163	.98	1.52	92.0	1.04	93.0	4.15	-----	-----	----	168	530	930	1,100
VT3	.2793	.0542	.0045	.3380	-----	-----	-----	-----	-----	-----	-----	.0173	1.373	.40	129	380	512	-----
VT4	.2828	.0542	.0045	.3415	-----	-----	-----	-----	-----	-----	-----	.0164	1.050	.38	128	355	506	-----
VT7	.2473	.0542	.0045	.3060	-----	-----	-----	-----	-----	-----	-----	-----	-----	----	131	355	510	-----

*Ailerons on wing models; rudders on vertical tail models.

**Control surfaces locked; values supplied by the model manufacturer.

TABLE II.- PHYSICAL CHARACTERISTICS OF MODIFIED WING MODELS

(a) Panels

Model	W_p , lb	W_f , lb	W_w , lb	W_t , lb	I_f , in-lb-sec ²	I_p , in-lb-sec ²	I_t , in-lb-sec ²	r , in.	l , in.
W2A	0.1085	0.0228	0.0039	0.1342	29.5×10^{-5}	72.6×10^{-5}	102.2×10^{-5}	-0.19	1.82
*W5A	.1075	.0239	.0039	.1353	25.1	83.2	108.3	.12	2.05
*W6A	.1180	.0239	.0039	.1458	25.1	79.3	104.5	.13	2.10

*Aileron locked.

(b) Mounts

Model	W_m , lb	I_m , in-lb-sec ²	W_0 , lb	I_0 , in-lb-sec ²
W2A	0.1823	95.3×10^{-5}	-----	-----
W2A1	-----	-----	0.2882	224.8×10^{-5}
W2A2	-----	-----	.2634	211.1
W2A3	-----	-----	.3110	261.0
W2A4	-----	-----	.2360	167.0
WSA	.1816	93.2	-----	-----
W5A1	-----	-----	.2882	218.5
W6A	.1816	93.2	-----	-----
W6A1	-----	-----	.2882	218.5
W6A2	-----	-----	.2667	195.8
W6A3	-----	-----	.3143	269.0
W6A4	-----	-----	.2408	148.2

TABLE III.- TYPICAL WEIGHT AND INERTIA DISTRIBUTION AND STRIP STATIC

UNBALANCE OF WING AND HORIZONTAL-TAIL MODELS

(a) Typical wing without aileron (model W1). Stations defined in figure 5(a).

Spanwise station -										Remarks
Flange	1	2	3	4	5	6	7	8	9	
Weight distribution (after compensating for cuttings), lb										
-----	62.30×10^{-4}	23.50×10^{-4}	21.36×10^{-4}	12.55×10^{-4}	15.72×10^{-4}	7.78×10^{-4}	6.16×10^{-4}	5.29×10^{-4}	3.59×10^{-4}	Chordwise station 1
227.70×10^{-4}	200.70	112.90	90.80	69.70	38.57	29.75	21.50	17.60	12.05	Chordwise station 2
-----	82.50	39.40	71.60	17.17	13.04	7.29	8.52	6.55	6.81	Chordwise station 3
Chordwise strip inertias, in-lb-sec ²										
37.0×10^{-6}	199.2×10^{-6}	81.2×10^{-6}	63.0×10^{-6}	22.9×10^{-6}	16.24×10^{-6}	7.07×10^{-6}	4.66×10^{-6}	3.01×10^{-6}	1.48×10^{-6}	About axis through strip center of gravity parallel to pitch axis
195.6	329.2	86.7	80.5	46.7	46.7	45.3	56.9	60.3	66.8	About pitch axis
Strip static unbalance about pitch axis*, in-lb										
375.0×10^{-4}	408.0×10^{-4}	60.6×10^{-4}	-112.2×10^{-4}	-94.9×10^{-4}	-88.3×10^{-4}	-80.5×10^{-4}	-84.8×10^{-4}	-77.6×10^{-4}	-74.2×10^{-4}	

*Based on actual strip weights and positive when strip center of gravity is forward of pitch axis.

TABLE III.- TYPICAL WEIGHT AND INERTIA DISTRIBUTION AND STRIP STATIC

UNBALANCE OF WING AND HORIZONTAL-TAIL MODELS - Continued

(b) Typical wing with aileron (model W4). Stations defined in figure 5(b).

Spanwise station -										Remarks
Flange	1	2	3	4	5	6	7	8	9	
Weight distribution (after compensating for cuttings), lb										
-----	54.30×10^{-4}	25.88×10^{-4}	21.05×10^{-4}	12.18×10^{-4}	20.73×10^{-4}	9.36×10^{-4}	8.98×10^{-4}	8.02×10^{-4}	3.72×10^{-4}	Chordwise station 1
238.50×10^{-4}	198.50	125.50	93.80	57.90	42.00	31.93	24.33	18.15	10.47	Chordwise station 2
-----	73.30	*75.55	121.00	*61.80	18.04	7.00	14.00	12.98	5.87	Chordwise station 3
Chordwise strip inertias, in-lb-sec ²										
41.15×10^{-6}	185.5×10^{-6}	* 74.4×10^{-6}	50.4×10^{-6}	* 19.0×10^{-6}	18.85×10^{-6}	7.28×10^{-6}	7.75×10^{-6}	4.30×10^{-6}	1.61×10^{-6}	About axis through strip center of gravity parallel to pitch axis
200.3	449.3	*76.6	76.6	*71.6	53.9	45.7	79.1	87.6	59.7	About pitch axis
Strip static unbalance about pitch axis**, in-lb										
372.0×10^{-4}	373.5×10^{-4}	89.8×10^{-4}	-154.2×10^{-4}	-127.4×10^{-4}	-103.2×10^{-4}	-83.9×10^{-4}	-113.3×10^{-4}	-111.5×10^{-4}	-67.0×10^{-4}	

*Hinges and screws attached.

**Based on actual strip weights and positive when strip center of gravity is forward of pitch axis.

Aileron mass 73.1
 Aileron moment of inertia about axis through its center of gravity and parallel to hinge line . . . 2.23
 Aileron moment of inertia about hinge line 4.40

TABLE III.- TYPICAL WEIGHT AND INERTIA DISTRIBUTION AND STRIP STATIC

UNBALANCE OF WING AND HORIZONTAL-TAIL MODELS - Concluded

(c) Typical horizontal tail (model HT5). Stations defined in figure 5(c).

Spanwise stations -							Remarks
Flange	1	2	3	4	5	6	
Weight distribution (after compensating for cuttings), lb							
-----	64.25×10^{-4}	38.33×10^{-4}	51.95×10^{-4}	16.95×10^{-4}	11.90×10^{-4}	11.45×10^{-4}	Chordwise station 1
182.40×10^{-4}	168.20	133.40	107.00	85.20	58.20	34.90	Chordwise station 2
-----	78.90	17.57	17.35	16.07	15.08	5.81	Chordwise station 3
Chordwise strip inertias, in-lb-sec ²							
8.81×10^{-6}	143.3×10^{-6}	49.7×10^{-6}	36.2×10^{-6}	14.22×10^{-6}	7.44×10^{-6}	2.88×10^{-6}	About axis through strip center of gravity parallel to pitch axis
9.09	146.1	68.4	111.3	181.6	226.8	196.0	About pitch axis
Strip static unbalance about pitch axis*, in-lb							
-143.5×10^{-4}	-58.3×10^{-4}	-116.0×10^{-4}	-225.0×10^{-4}	-275.3×10^{-4}	-267.2×10^{-4}	-196.0×10^{-4}	

*Based on actual strip weights and positive when strip center of gravity is forward of pitch axis.

TABLE IV.- REPRESENTATIVE MODE SHAPES OF WING MODELS

[Deflections normalized on maximum deflection]

(a) $K = 4,075$ in-lb/radian

Chord, percent (*)	Span, percent								
	0	10	30	40	50	60	70	90	100
$f_1 = 138$ cps									
0	-0.050	-0.045	-0.010	0.032	0.085	0.156	0.245	0.528	0.750
25	-.035	-.024	.030	.075	.135	.210	.300	.600	.810
50	-.010	.005	.075	.128	.188	.266	.362	.677	.873
75	.014	.041	.125	.186	.245	.326	.435	.755	.920
100	.040	.081	.175	.235	.302	.395	.512	.835	1.000
$f_2 = 392$ cps									
0	0.005	0	-0.035	-0.079	-0.186	-0.300	-0.317	0.079	0.462
25	0	-.010	-.070	-.140	-.239	-.286	-.273	.200	.604
50	-.010	-.028	-.117	-.207	-.276	-.269	-.204	.335	.742
75	-.028	-.055	-.197	-.275	-.304	-.248	-.095	.473	.884
100	-.055	-.096	-.317	-.345	-.324	-.224	.065	.616	1.000
$f_3 = 648$ cps									
0	-0.183	-0.137	0.061	0.351	0.718	0.810	0.802	0.802	0.802
25	-.084	-.038	.122	.351	.634	.740	.763	.763	.580
50	-.031	-.015	-.038	-.046	.084	.336	.519	.382	-.305
75	-.069	-.168	-.611	-.651	-.641	-.596	-.588	-.702	-.840
100	-.244	-.763	-.939	-.940	-.962	-.970	-.984	-1.000	-1.000

*Chordwise stations based on chord lengths not including leading-edge extension.

(b) $K = 9,770$ in-lb/radian

Chord, percent (*)	Span, percent								
	0	10	30	40	50	60	70	90	100
$f_1 = 142$ cps									
0	-0.025	-0.019	0.016	0.057	0.121	0.204	0.312	0.637	0.860
25	-.019	-.006	.046	.096	.166	.255	.376	.692	.892
50	-.006	.015	.083	.147	.223	.325	.448	.747	.925
75	.015	.047	.136	.206	.296	.404	.525	.806	.962
100	.038	.072	.199	.280	.376	.479	.605	.863	1.000
$f_2 = 399$ cps									
0	0.094	0.067	-0.023	-0.077	-0.157	-0.229	-0.254	0.143	0.429
25	.067	.029	-.071	-.137	-.214	-.250	-.226	.286	.572
50	.031	-.017	-.143	-.212	-.267	-.263	-.172	.429	.714
75	-.009	-.076	-.243	-.300	-.309	-.267	-.074	.572	.858
100	-.069	-.157	-.371	-.400	-.340	-.257	.074	.714	1.000
$f_3 = 654$ cps									
0	-0.500	-0.429	0.157	0.507	0.750	0.886	0.964	0.993	1.000
25	-.272	-.186	.157	.457	.700	.814	.872	.857	.714
50	-.057	-.079	-.257	-.279	0	.572	.657	.507	-.772
75	-.143	-.343	-.700	-.722	-.729	-.729	-.743	-.757	-.886
100	-.643	-.857	-.943	-.950	-.964	-.971	-.979	-.986	-.986

*Chordwise stations based on chord lengths not including leading-edge extension.

TABLE V.- SUMMARY OF MASS, INERTIA, AND PITCH STIFFNESS VARIATIONS
FOR VARIOUS CONFIGURATIONS OF WING MODELS

Original (reworked) model configuration			Modified model configuration			
W_m , lb	I_m , in-lb-sec ²	K , in-lb/radian	W_0 , lb	I_0 , in-lb-sec ²	Calculated K_0 , in-lb/radian	Measured K_0 , in-lb/radian
W2A			W2A-1			
0.1823	95.3×10^{-5}	3,840	0.2882	225.0×10^{-5}	6,090	6,150
.1823	95.3	6,000	.2882	225.0	9,500	9,580
.1823	95.3	6,100	.2882	225.0	9,560	9,750
.1823	95.3	7,600	.2882	225.0	11,720	11,900
.1823	95.3	7,710	.2882	225.0	11,930	12,050
W2A			W2A-2			
0.1823	95.3×10^{-5}	6,000	0.2634	211.2×10^{-5}	9,130	9,080
W2A			W2A-3			
0.1823	95.3×10^{-5}	6,000	0.3110	261.0×10^{-5}	10,470	10,850
W2A			W2A-4			
0.1823	95.3×10^{-5}	6,000	0.2360	167.0×10^{-5}	7,940	8,000
W5A			W5A-1			
0.1816	93.2×10^{-5}	3,870	0.2882	218.7×10^{-5}	5,780	5,880
.1816	93.2	6,060	.2882	218.7	9,010	8,900
.1816	93.2	7,580	.2882	218.7	10,950	10,860
W6A			W6A-1			
0.1816	93.2×10^{-5}	460	-----	-----	-----	-----
.1816	93.2	2,500	-----	-----	-----	-----
.1816	93.2	6,000	0.2882	218.7×10^{-5}	8,660	8,500
W6A			W6A-2			
0.1816	93.2×10^{-5}	6,000	0.2667	195.8×10^{-5}	8,180	8,200
W6A			W6A-3			
0.1816	93.2×10^{-5}	6,000	0.3143	269.0×10^{-5}	9,730	9,800
W6A			W6A-4			
0.1816	93.2×10^{-5}	6,000	0.2408	148.2×10^{-5}	7,170	7,200

TABLE VI.- EXPERIMENTAL RESULTS OF FIRST PHASE OF INVESTIGATION

(a) Wing models

Model	Run	K, in-lb/radian	K _c , in-lb/radian	f ₁ , cps	f ₂ , cps	f ₃ , cps	f ₄ , cps	f ₅ , cps	M	q, lb/sq ft	ρ, slugs/cu ft	a, ft/sec	f _f , cps	Remarks
W6	16	18,400	28.75	137	335	440	555	730	1.30	3,460	0.00409	998	---	Maximum conditions; no flutter
W6	6	18,400	28.75	138	352	460	559	743	1.64	3,470	.00298	930	---	Maximum conditions; no flutter
W6	10	18,400	28.75	137	350	458	560	740	2.00	3,515	.00236	862	---	Maximum conditions; no flutter
W6	12	18,400	28.75	137	349	451	559	735	2.55	3,180	.00152	790	---	Maximum conditions; no flutter
W6	20	18,400	22.2	137	326	435	553	710	1.30	3,395	.00408	993	---	Maximum conditions; no flutter
W6	26	18,400	20.3	137	323	430	550	725	1.64	3,576	.00308	928	---	Maximum conditions; no flutter
W5	35	17,300	28.0	128	332	445	555	730	1.30	3,215	.00384	995	---	Maximum conditions; no flutter
W5	36	17,300	6.0	126	375	533	675	870	1.30	3,215	.00384	995	---	Maximum conditions; no flutter
W5	45	17,300	2.7	118	370	526	675	820	1.30	1,800	.00220	984	400	Aileron fluttered; limited amplitude
W5	42	17,300	5.7	127	375	520	679	850	1.64	3,800	.00350	930	---	Maximum conditions; no flutter
W5	38	17,300	28.0	126	375	533	675	870	2.00	3,800	.00250	880	---	Maximum conditions; no flutter
W5	39	17,300	6.0	127	382	555	695	850	2.00	3,800	.00250	880	---	Lost aileron in opening shock
W3	30	18,400	19.62	128	316	400	552	665	1.30	3,520	.00414	1,000	---	Maximum conditions; no flutter
W3	32	16,500	17.7	125	308	410	555	720	1.30	3,380	.00414	982	---	Maximum conditions; no flutter
W3	33	17,300	14.4	125	285	383	534	667	1.30	3,140	.00375	995	---	Maximum conditions; no flutter
W3	34	17,300	6.0	125	367	520	620	720	1.30	3,185	.00380	995	---	Maximum conditions; no flutter
W3	28	18,400	19.62	128	318	402	552	662	1.64	3,505	.00302	928	---	Maximum conditions; no flutter
W2	5	18,400	-----	147	390	540	685	850	1.64	3,820	.00323	938	---	Maximum conditions; no flutter
W4	93	10,850	28.75	129	356	430	534	633	1.30	3,300	.00390	1,000	310	Maximum conditions; no flutter

TABLE VI.- EXPERIMENTAL RESULTS OF FIRST PHASE OF INVESTIGATION - Continued

(b) Horizontal-tail models

Model	Run	K, in-lb/radian	f ₁ , cps	f ₂ , cps	f ₃ , cps	f ₄ , cps	f ₅ , cps	M	q, lb/sq ft	ρ, slugs/cu ft	a, ft/sec	f _f , cps	Remarks
HT-1	14	2,310	131	394	610	867	1,000	1.30	3,500	0.00414	1,000	---	Maximum conditions; no flutter
HT-1	2	2,310	133	406	625	855	980	1.64	3,780	.00317	940	---	Maximum conditions; no flutter
HT-1	8	2,310	133	408	625	880	1,000	2.00	3,400	.00229	862	---	Maximum conditions; no flutter
HT-1	11	2,310	133	400	621	872	1,000	2.55	2,970	.00152	780	---	Maximum conditions; no flutter
HT-1	18	1,890	132	392	625	860	1,033	1.30	3,500	.00413	1,000	---	Maximum conditions; no flutter
HT-1	21	1,440	122	374	601	868	1,000	1.30	3,585	.00432	1,000	---	Maximum conditions; no flutter
HT-1	25	1,440	122	373	600	870	-----	1.64	3,815	.00324	936	---	Maximum conditions; no flutter
HT-5	43	2,260	133	415	625	912	1,060	1.30	3,000	.00358	995	---	Low damping; 325 cps
HT-5	41	2,260	133	415	625	912	1,060	1.64	3,800	.00350	936	---	Maximum conditions; no flutter
HT-5	40	2,260	133	408	621	912	1,080	2.00	3,800	.00250	873	---	Maximum conditions; no flutter
HT-5	44	1,432	121	375	588	900	1,012	1.30	2,905	.00345	1,000	---	Low damping; 300 cps
HT-5	44	1,432	121	375	588	900	1,012	1.30	3,225	.00378	1,003	300	Constant amplitude flutter
HT-5	46	1,174	117	365	555	879	1,012	1.30	2,940	.00348	1,000	284	Destructive flutter
HT-4	22	1,440	126	377	594	875	-----	1.30	2,815	.00339	990	305	Divergent flutter

TABLE VI.- EXPERIMENTAL RESULTS OF FIRST PHASE OF INVESTIGATION - Concluded

(c) Vertical-tail models

Model	Run	K_c , in-lb/radian	f_1 , cps	f_2 , cps	f_3 , cps	f_4 , cps	f_5 , cps	M	q , lb/sq ft	ρ , slugs/cu ft	a , ft/sec	f_f , cps	Remarks
VT-7	91	-----	129	355	510	692	1,000	1.30	2,610	0.00316	990	370	Low damping; 370 cps oscillations
VT-7	91	-----	129	355	510	692	1,000	1.30	3,395	.00406	994	---	Maximum tunnel
VT-4	94	136.5	129	356	430	534	633	1.30	2,540	.00306	994	360	Low damping; 360 cps oscillations
VT-4	94	136.5	129	356	430	534	633	1.30	3,500	.00415	1,000	---	Maximum tunnel
VT-4	95	136.5	131	354	438	538	650	1.64	2,725	.00235	930	360	Low damping; 360 cps oscillations
VT-4	95	136.5	131	354	438	538	650	1.64	3,810	.00326	932	---	Maximum tunnel
VT-4	97	136.5	128	358	427	542	645	2.00	3,800	.00238	894	---	Maximum tunnel; no flutter
VT-4	98	136.5	128	358	427	542	645	2.55	3,055	.00151	790	---	Maximum tunnel; no flutter
VT-4	99	65.6	128	348	381	521	628	1.30	3,072	.00368	995	360	Low damping; 360 cps oscillations
VT-4	99	65.6	128	348	381	521	628	1.30	3,470	.00414	997	---	Maximum tunnel
VT-4	100	52.3	128	355	506	600	650	1.30	2,180	.00262	990	360	Low damping; 360 cps oscillations
VT-4	100	52.3	128	355	506	600	650	1.30	3,470	.00407	1,000	---	Maximum tunnel
VT-3	101	99.2	127	348	374	584	690	1.30	2,505	.00302	991	360	Low damping; 360 cps oscillations
VT-3	101	99.2	127	348	374	584	690	1.30	3,470	.00414	996	---	Maximum tunnel
VT-3	102	99.2	127	350	373	586	700	1.30	3,530	.00425	990	360	Low damping; 360 cps oscillations
VT-3*	104	99.2	137	356	386	585	600	1.30	3,500	.00422	990	350	Low damping; 350 cps oscillations

*Radar mass removed.

TABLE VII.- EXPERIMENTAL RESULTS OF SECOND PHASE OF INVESTIGATION

Model	Run	K, in-lb/radian	f ₁ , cps	f ₂ , cps	f ₃ , cps	f ₄ , cps	f ₅ , cps	M	q, lb/sq ft	ρ, slugs/cu ft	a, ft/sec	f _f , cps	Remarks
W1	67	11,100	140	390	654	804	1,000	1.30	3,485	0.00461	1,000	340	Constant amplitude flutter
W1	47	9,710	147	398	675	825	1,000	1.30	2,990	.00359	993	323	Divergent flutter
W1	68	8,700	142	394	654	804	1,000	1.30	2,510	.00334	995	300	Divergent flutter
W1	54	7,820	144	402	660	817	1,000	1.30	2,090	.00251	993	275	Divergent flutter
W1	52	6,010	143	404	650	820	1,000	1.30	1,365	.00166	986	250	Divergent flutter
W1	70	4,085	138	395	643	808	1,000	1.30	967	.00120	978	213	Divergent flutter
W1	71	3,290	124	368	632	750	940	1.30	698	.00095	983	188	Divergent flutter
W1	72	2,535	128	390	640	795	990	1.30	463	.00064	976	176	Divergent flutter
W1	63	11,100	140	396	650	805	1,000	1.64	3,540	.00301	936	340	Low damping
W1	66	9,745	142	392	653	816	998	1.64	3,440	.00292	934	330	Divergent flutter
W1	62	9,770	142	394	650	810	990	1.64	3,458	.00293	937	320	Divergent flutter
W1	61	9,150	140	393	650	805	1,000	1.64	3,130	.00267	934	310	Divergent flutter
W1	60	8,020	139	390	650	805	1,000	1.64	2,690	.00234	927	286	Divergent flutter
W1	59	7,080	145	400	660	815	1,000	1.64	2,282	.00201	920	260	Divergent flutter
W1	75	5,425	135	383	646	780	980	1.64	1,693	.00149	921	228	Divergent flutter
W1	74	3,265	133	386	632	785	985	1.64	808	.00072	911	194	Divergent flutter
W1	73	2,535	128	390	640	795	990	1.64	555	.00050	910	174	Divergent flutter
W1	78	8,900	134	384	636	786	960	2.00	3,725	.00243	876	314	Low damping
W1	79	7,550	134	385	622	784	960	2.00	3,300	.00218	869	292	Divergent flutter
W1	81	6,525	130	382	620	790	960	2.00	2,600	.00176	860	256	Divergent flutter
W1	82	3,955	126	377	606	786	975	2.00	1,370	.00094	853	208	Divergent flutter; model broke
W2	85	6,525	131	375	650	784	975	2.00	3,780	.00243	880	278	Barely fluttered
W2	84	4,980	136	380	650	806	975	2.00	2,157	.00146	861	244	Divergent flutter
W2	86	6,000	128	370	644	766	965	2.00	3,417	.00222	876	266	Divergent flutter
W2	83	3,955	138	393	650	814	990	2.00	1,475	.00101	857	220	Divergent flutter
W2	87	4,230	125	352	632	766	960	2.55	2,470	.00125	782	220	Divergent flutter
W2	89	4,750	130	367	638	770	950	2.55	3,128	.00152	796	236	Divergent flutter; model broke

TABLE VIII.- EXPERIMENTAL RESULTS OF THIRD PHASE OF INVESTIGATION

28

Model	Run	K, in-lb/radian	f ₁ , cps	f ₂ , cps	f ₃ , cps	f ₄ , cps	f ₅ , cps	M	q, lb/sq ft	ρ, slugs/cu ft	a, ft/sec	f _f , cps	Remarks
W2A	115	3,840	147	236	390	695	800	1.30	766	0.00094	984	210	Divergent flutter
W2A-1	116	6,150	144	225	387	680	785	1.30	838	.00102	984	206	Divergent flutter
W2A	107	6,000	150	400	705	830	1,045	1.30	1,512	.00186	981	260	Divergent flutter
W2A-1	112	9,580	149	392	686	800	1,015	1.30	1,527	.00187	980	246	Slowly divergent flutter
W2A	110	9,820	150	403	706	825	1,055	1.30	2,878	.00349	988	312	Slowly divergent flutter
W2A	113	7,710	150	395	685	805	1,030	1.30	2,245	.00266	999	288	Slowly divergent flutter
W2A-1	114	12,050	150	393	695	800	1,025	1.30	2,393	.00286	996	290	Slowly divergent flutter
W2A-4	119	8,000	148	380	690	784	1,025	1.30	1,835	.00222	989	266	Slowly divergent flutter
W2A-2	117	9,080	147	380	690	800	1,020	1.30	1,760	.00213	988	260	Divergent flutter
W2A-3	118	10,850	150	385	690	785	1,030	1.30	1,775	.00212	995	264	Slowly divergent flutter
W2A	123	6,100	149	386	685	790	1,005	1.64	1,772	.00155	923	260	Divergent flutter
W2A-1	125	9,750	147	384	680	800	1,020	1.64	1,895	.00167	919	260	Slowly divergent flutter
W2A	120	7,600	148	386	686	790	1,015	1.64	2,447	.00213	923	284	Slowly divergent flutter
W2A-1	122	11,900	148	378	690	780	1,015	1.64	3,080	.00265	930	294	Slowly divergent flutter
W5A	127	3,870	122	240	363	624	780	1.64	1,241	.00109	921	196	Divergent flutter
W5A-1	128	5,880	122	222	354	614	775	1.64	1,223	.00108	918	200	Divergent flutter
W5A	129	6,060	122	286	349	626	775	1.64	2,108	.00185	921	244	Divergent flutter
W5A-1	130	8,900	118	263	344	606	750	1.64	2,083	.00185	915	240	Divergent flutter
W5A	131	7,580	118	270	335	614	770	1.64	2,642	.00232	921	260	Divergent flutter
W5A-1	132	10,860	119	---	342	600	745	1.64	2,780	.00242	924	268	Divergent flutter
W6A	134	6,000	132	283	361	624	760	1.64	1,950	.00172	918	232	Divergent flutter
W6A-4	135	7,200	120	272	330	600	700	1.64	2,095	.00187	914	238	Divergent flutter
W6A-2	136	8,200	120	270	327	600	700	1.64	2,172	.00194	914	238	Divergent flutter
W6A-1	137	8,500	120	263	330	600	695	1.64	2,048	.00180	919	235	Divergent flutter
W6A-3	138	9,800	120	256	325	590	694	1.64	2,100	.00186	916	232	Divergent flutter
W6A-3	139	6,000	113	204	318	590	640	1.64	1,017	.00090	916	188	Divergent flutter
W6A	140	2,500	106	183	315	584	692	1.64	620	.00055	912	159	Divergent flutter
W6A	141	460	118	147	315	590	690	1.64	440	.00039	912	88	Divergent flutter

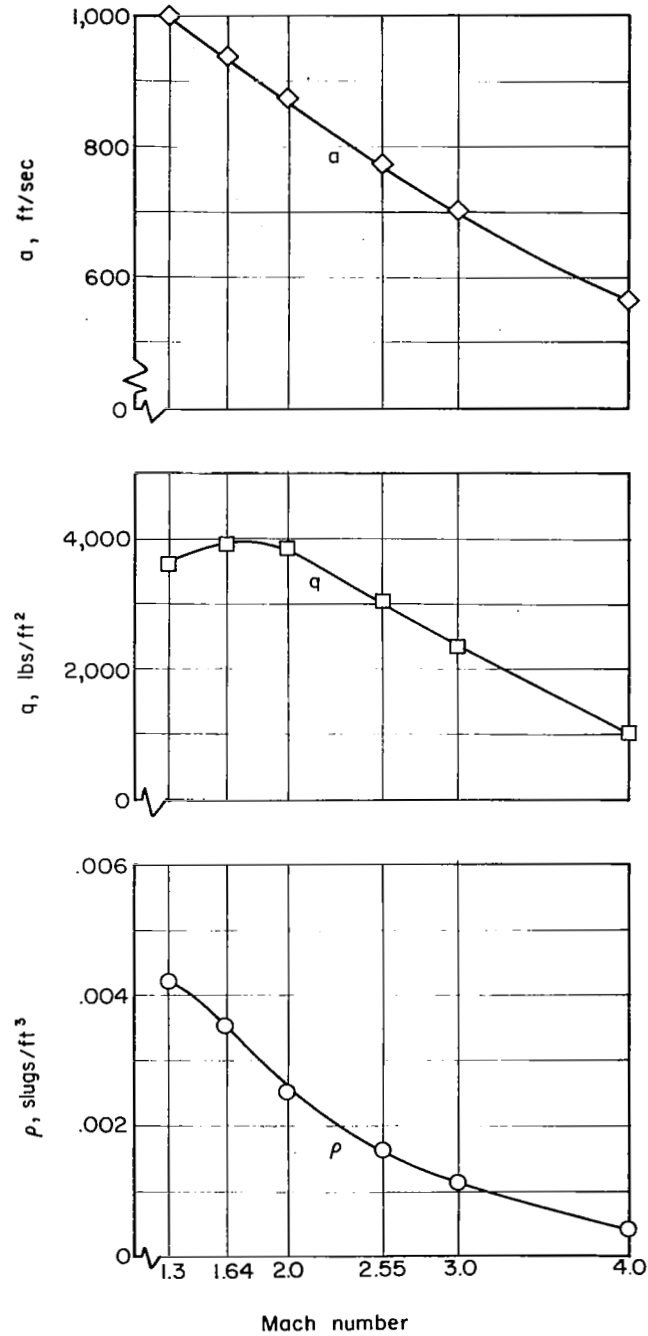
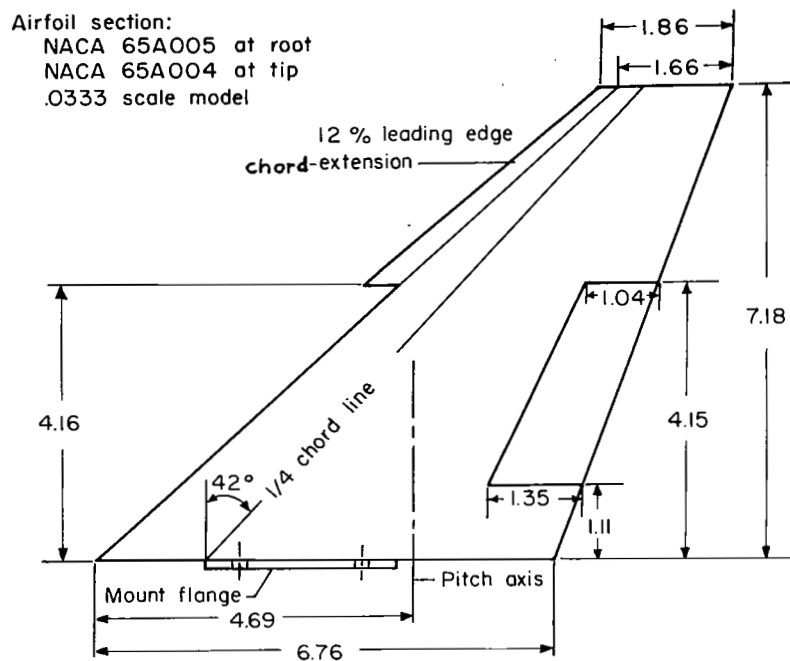
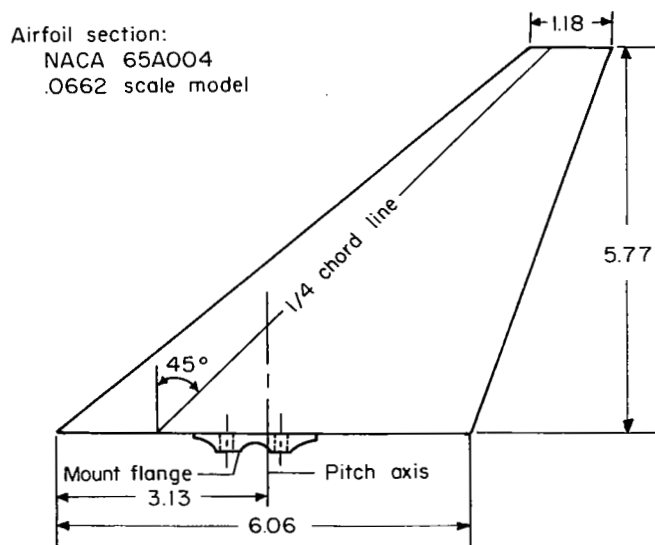


Figure 1.- Performance curves of the Langley 9- by 18-inch supersonic flutter tunnel showing maximum test-section conditions obtainable.

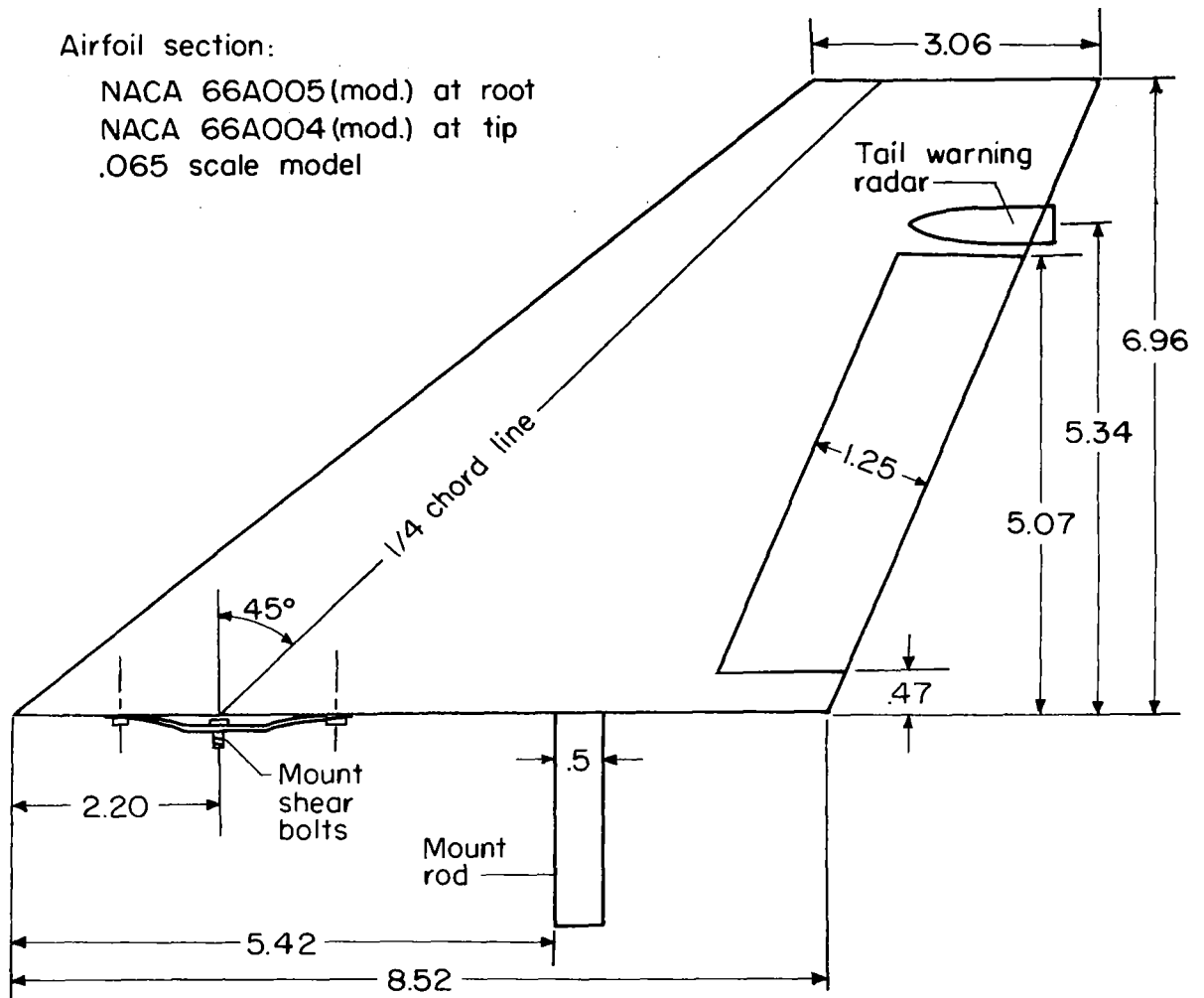


(a) Wing geometry.



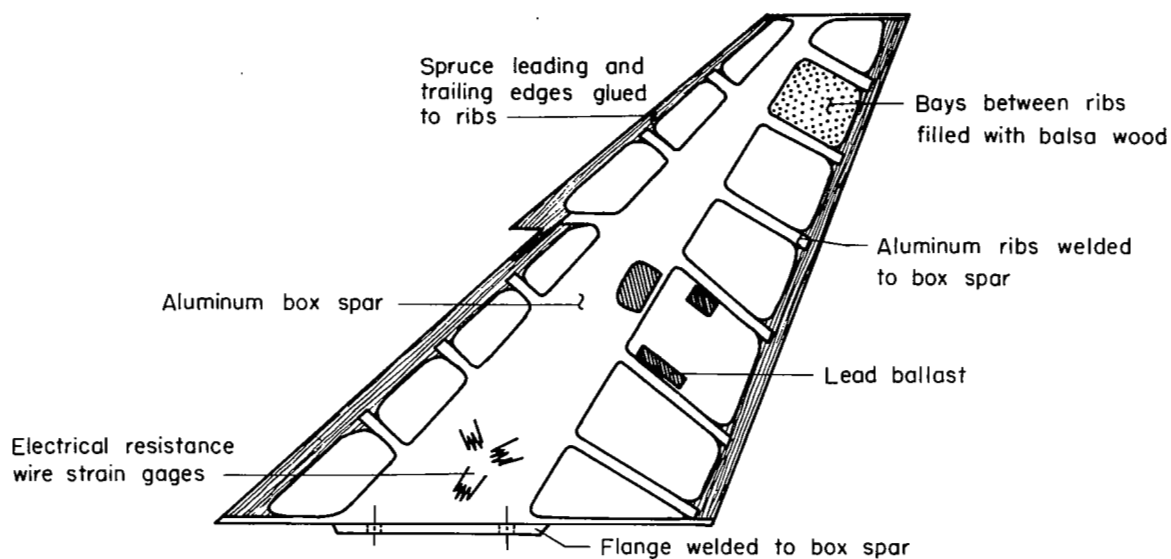
(b) Horizontal-tail geometry.

Figure 2.- Geometry of wing, horizontal-tail, and vertical-tail models. All dimensions are in inches.

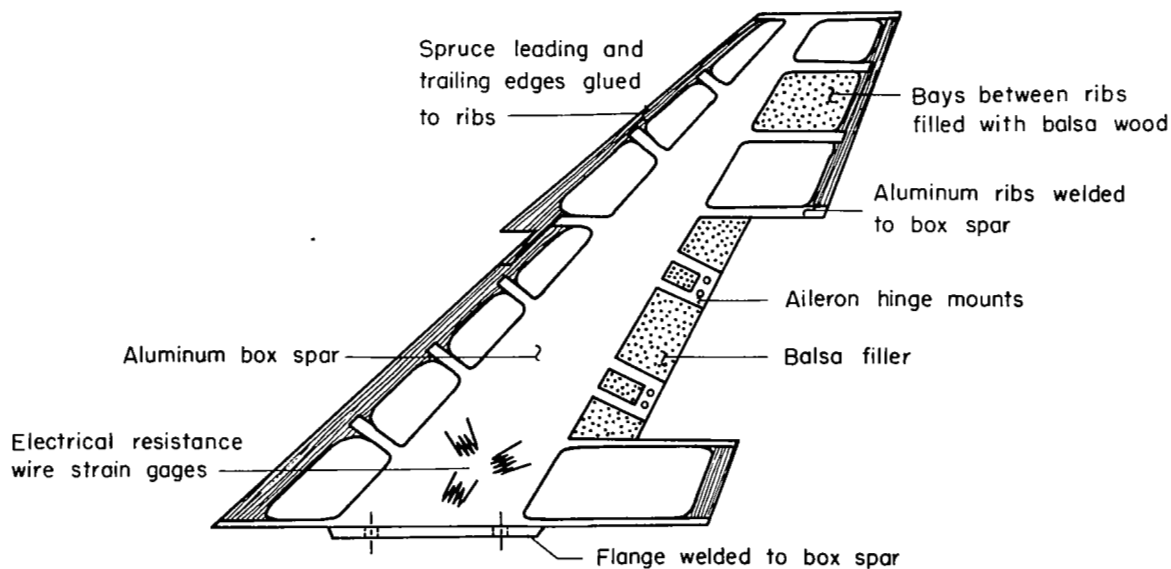


(c) Vertical-tail geometry.

Figure 2.- Concluded.

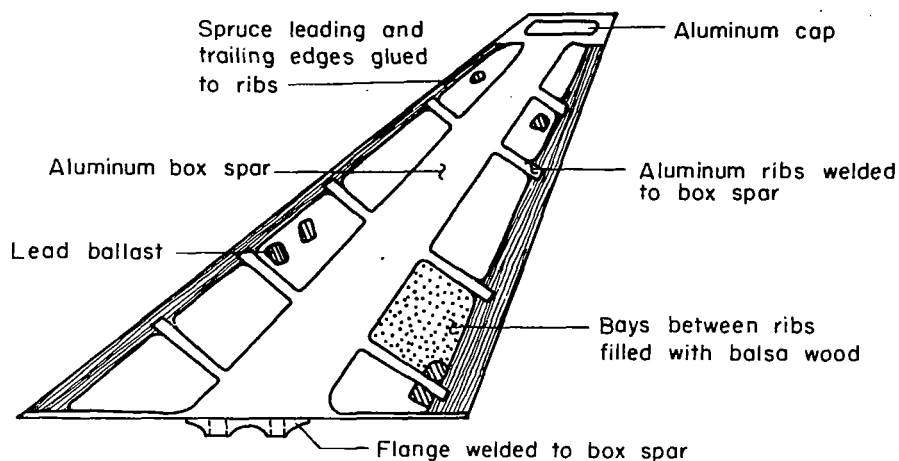


(a) Wing without aileron.

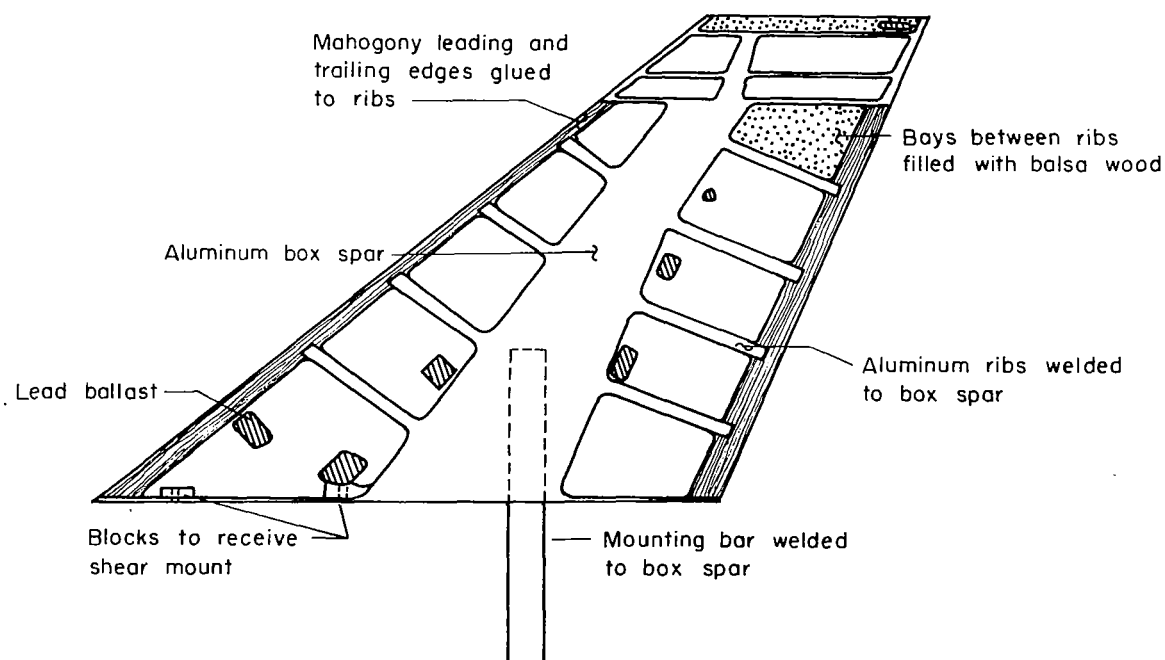


(b) Wing with aileron.

Figure 3.- Details of typical model construction.

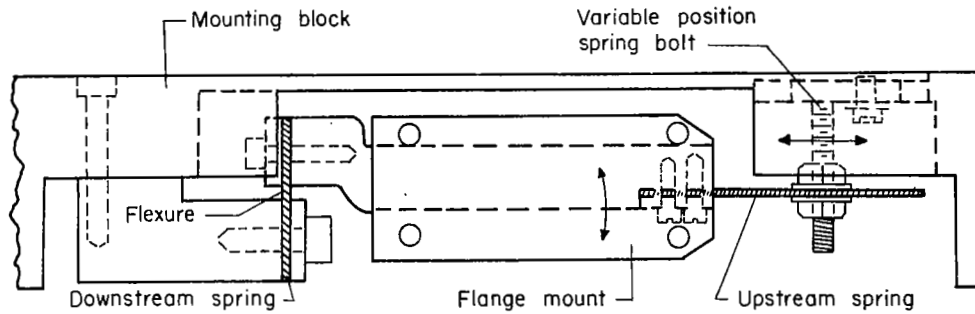


(c) Horizontal tail.

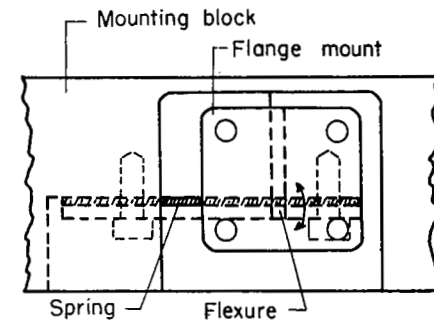


(d) Vertical tail.

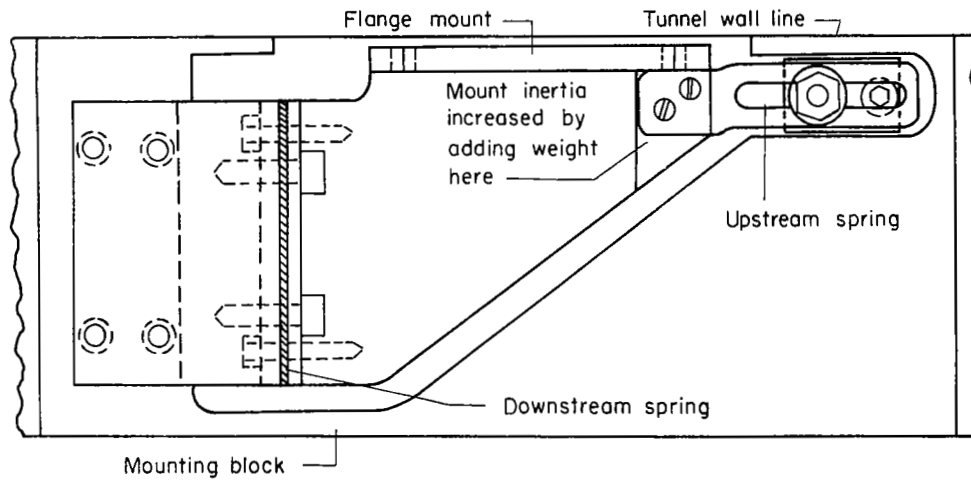
Figure 3.- Concluded.



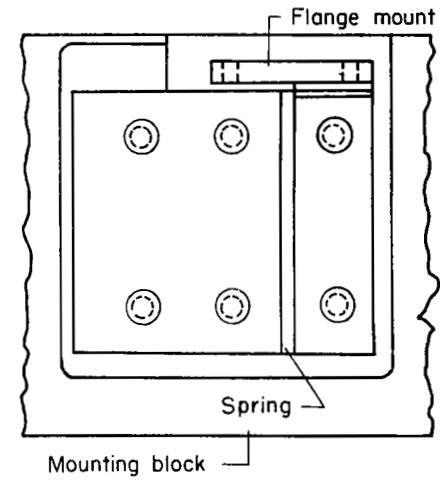
Side view



Side view



Top view

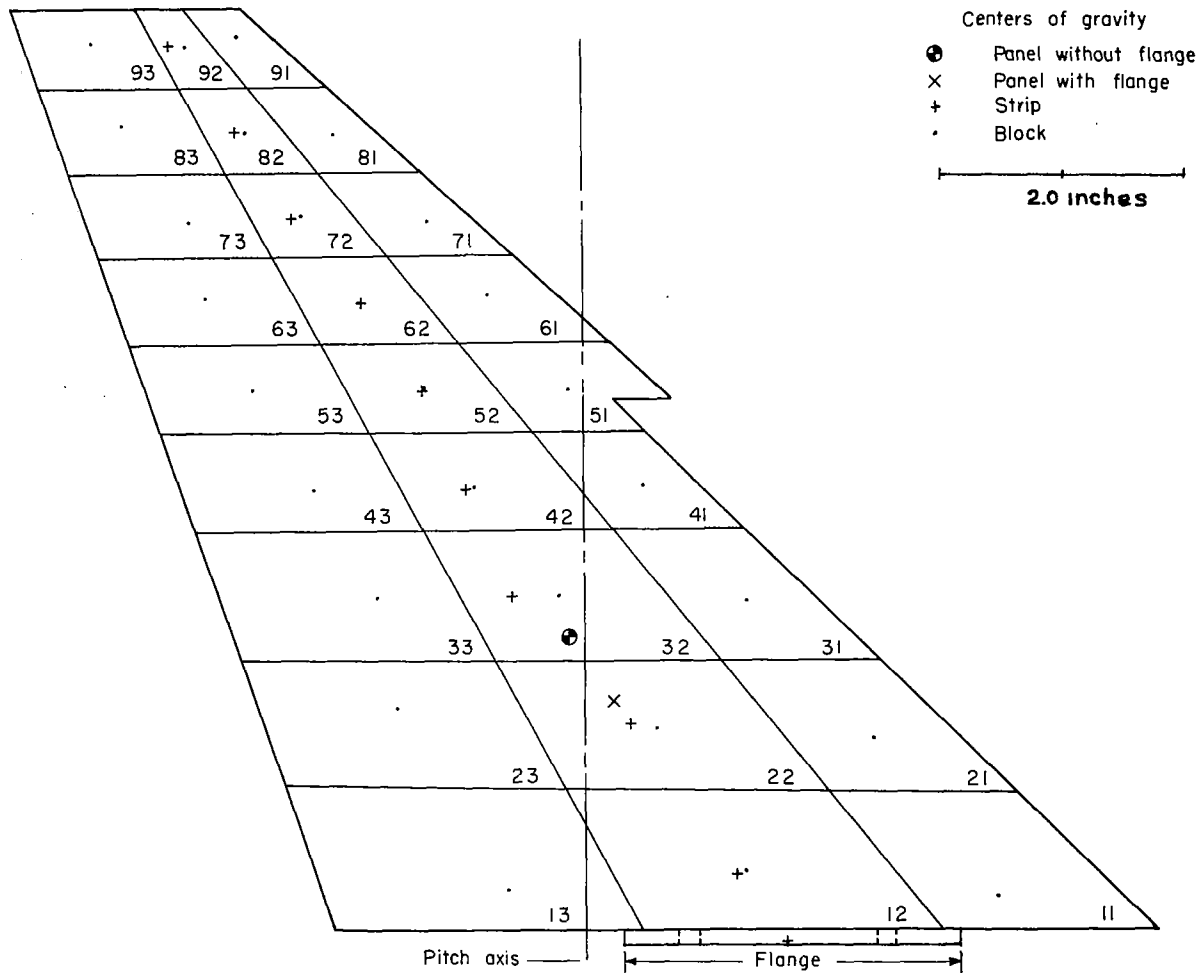


Top view

(a) Wing-mount assembly.

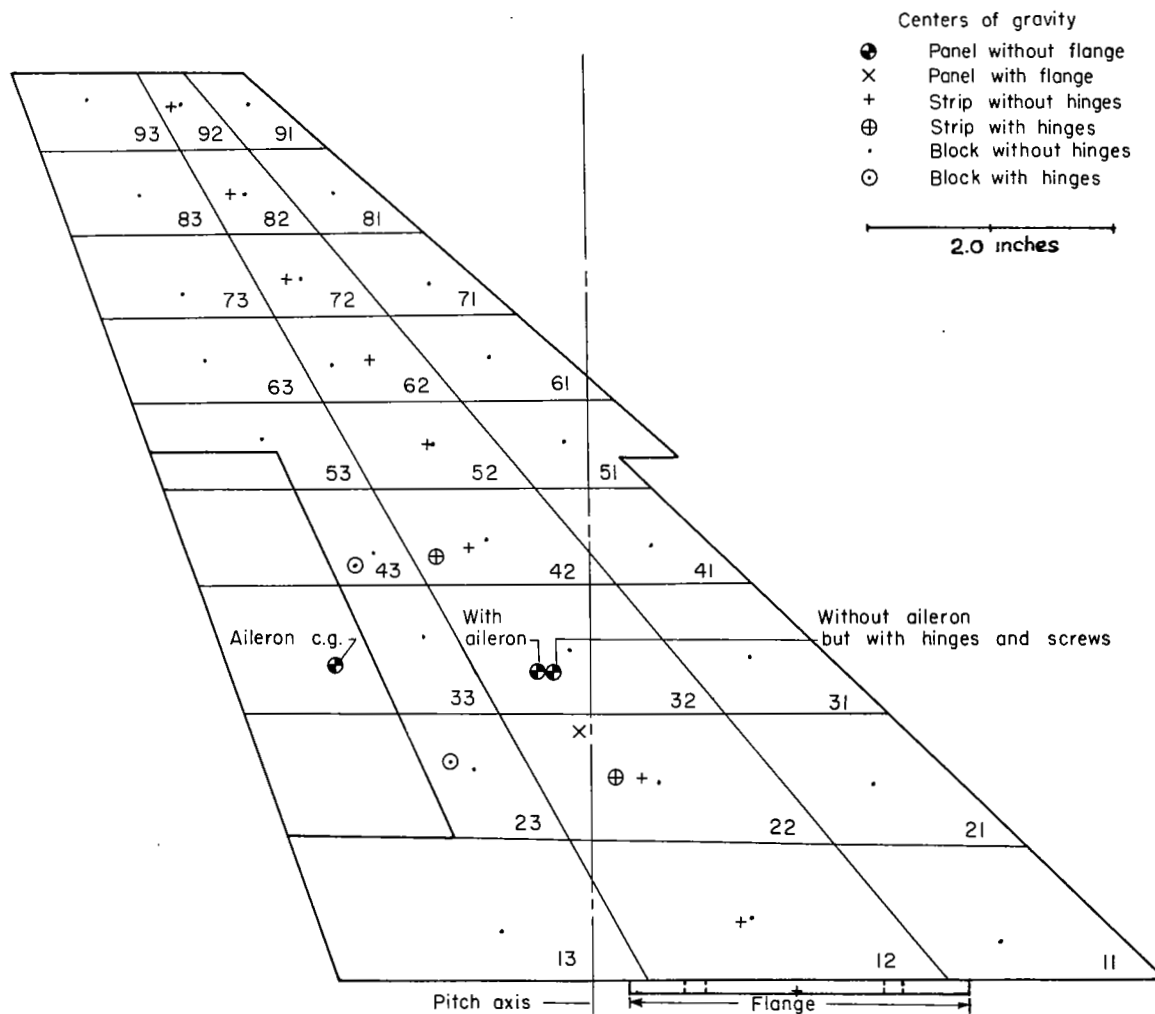
(b) Horizontal-tail-mount assembly.

Figure 4.- Mount assemblies for wings and horizontal tails.



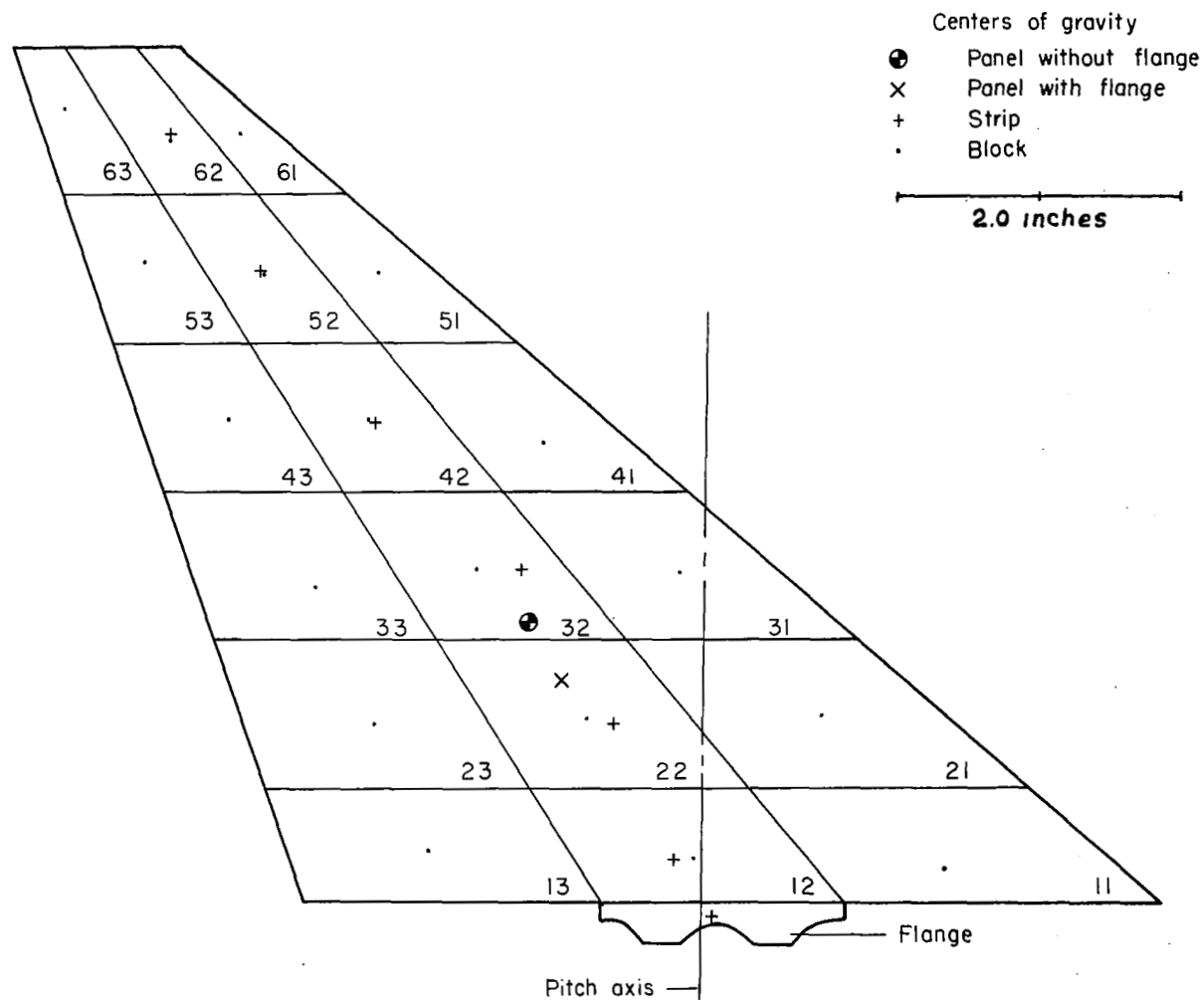
(a) Typical wing without aileron (wing model W1).

Figure 5.- Streamwise strip, block, and panel centers of gravity of typical wing and horizontal-tail models.



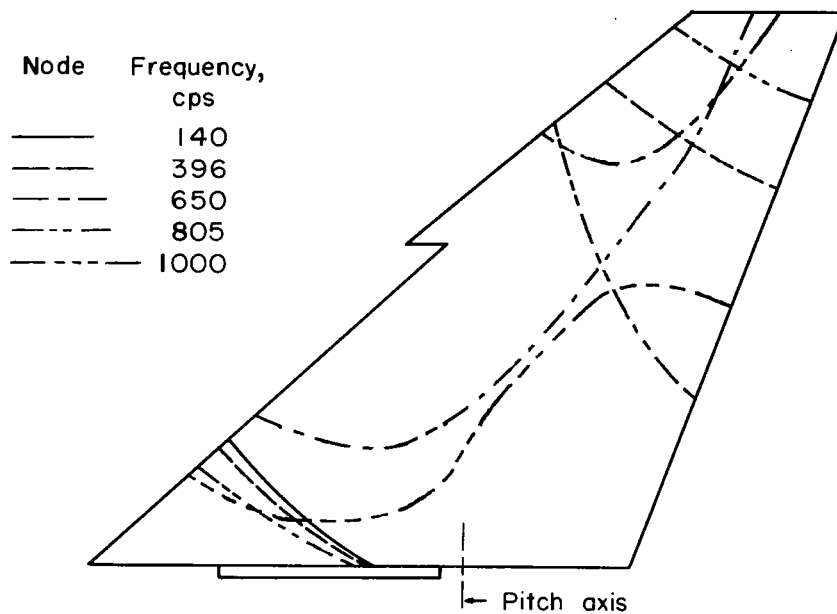
(b) Typical wing with aileron (model W4).

Figure 5.- Continued.

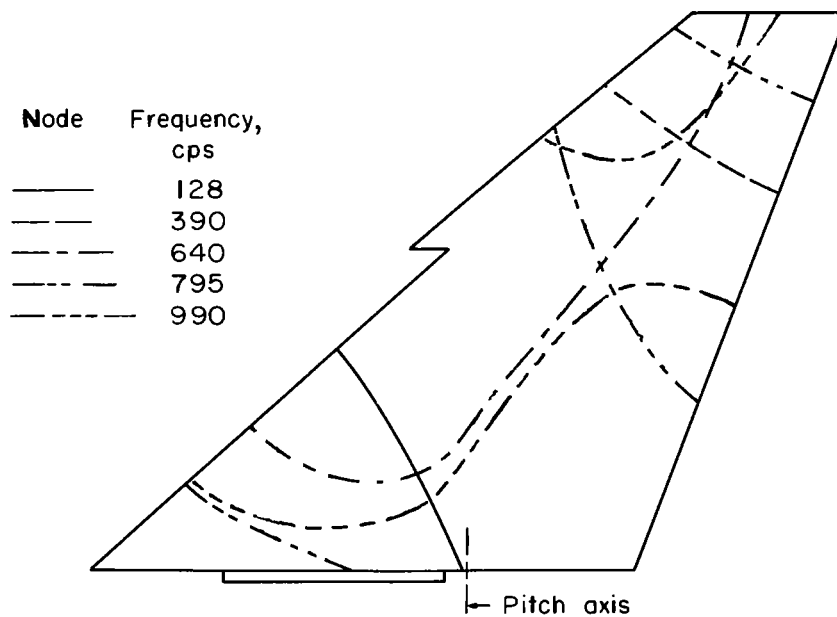


(c) Typical horizontal tail (model HT5).

Figure 5.- Concluded.

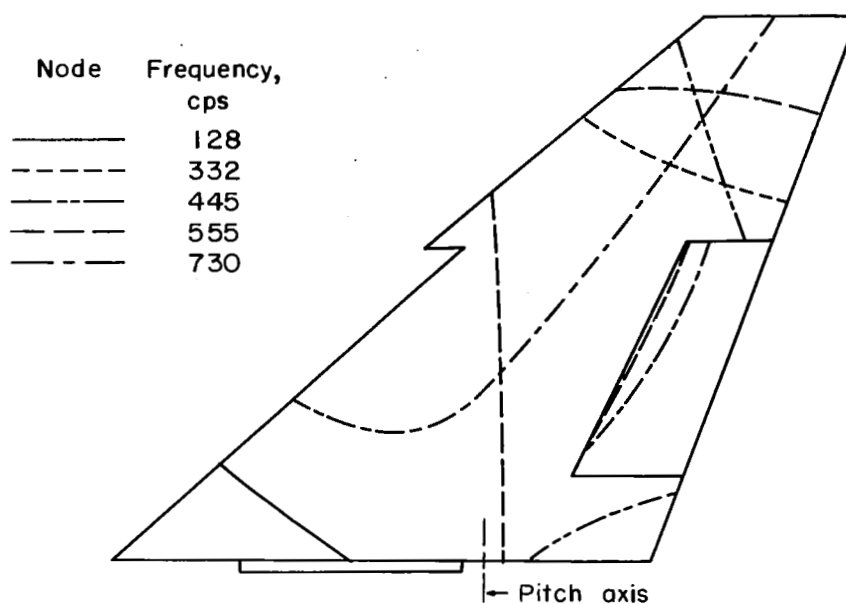


(a) Wing without aileron; $K = 11,000$ in-lb/radian, run 63.

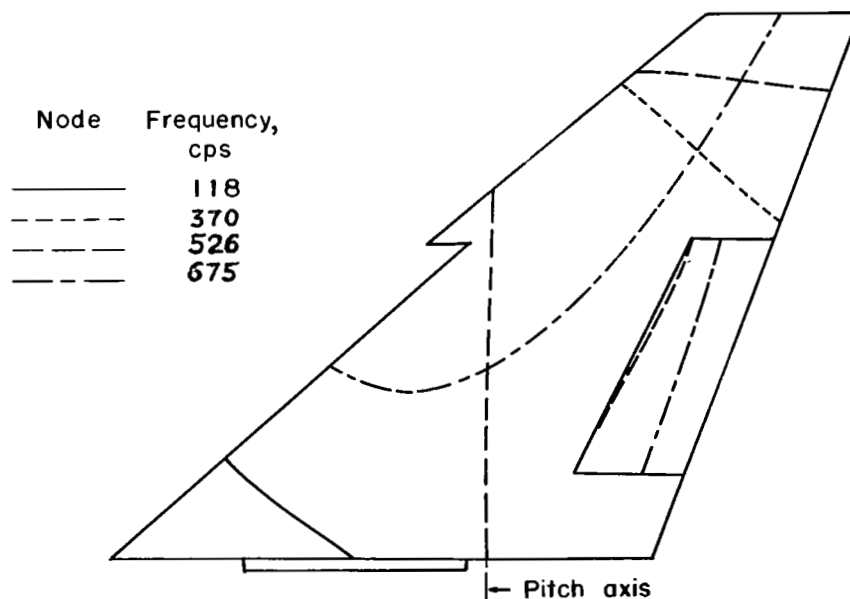


(b) Wing without aileron; $K = 2,535$ in-lb/radian, run 73.

Figure 6.- Typical model node lines for some representative pitch and control stiffnesses.

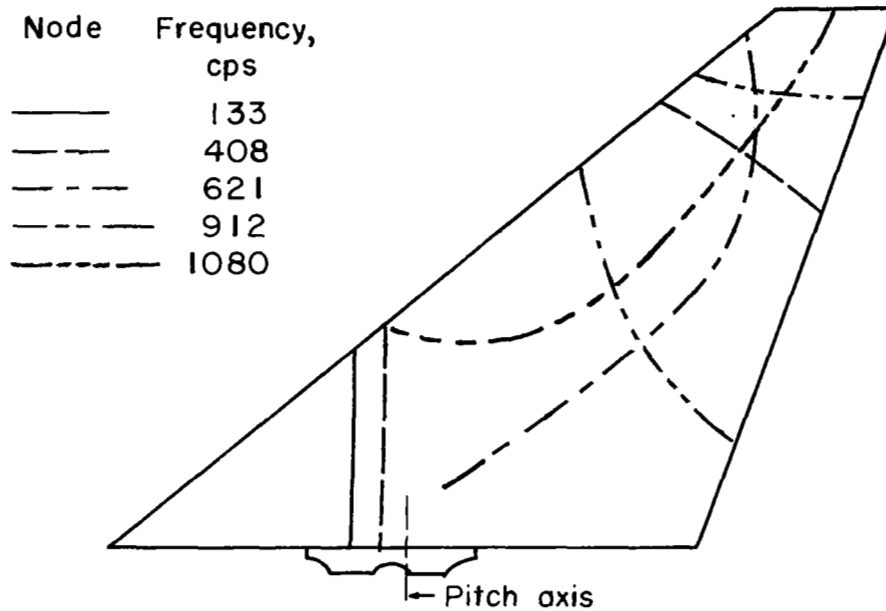


(c) Wing with aileron; $K = 17,300$ in-lb/radian; $K_c = 28.0$ in-lb/radian; run 35.

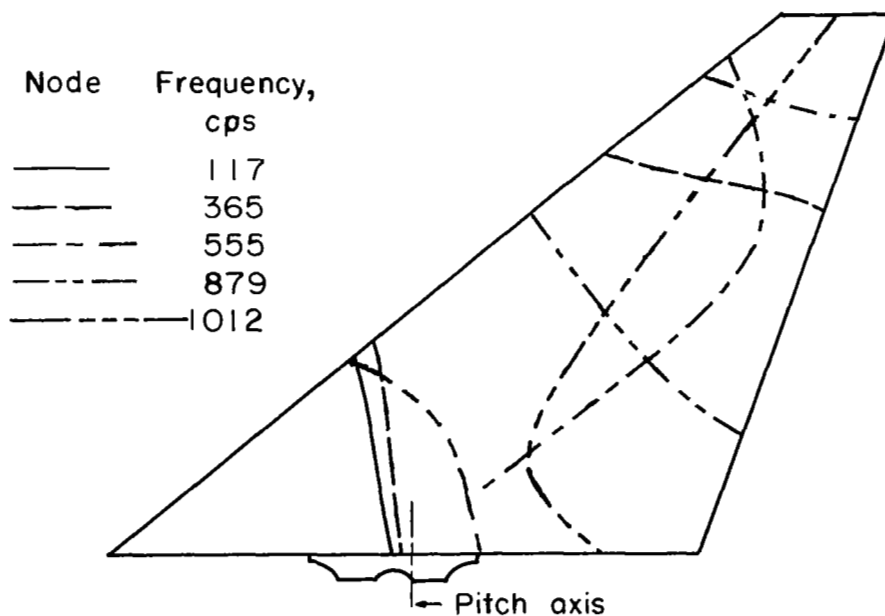


(d) Wing with aileron; $K = 17,300$ in-lb/radian; $K_c = 2.7$ in-lb/radian; run 45.

Figure 6.- Continued.

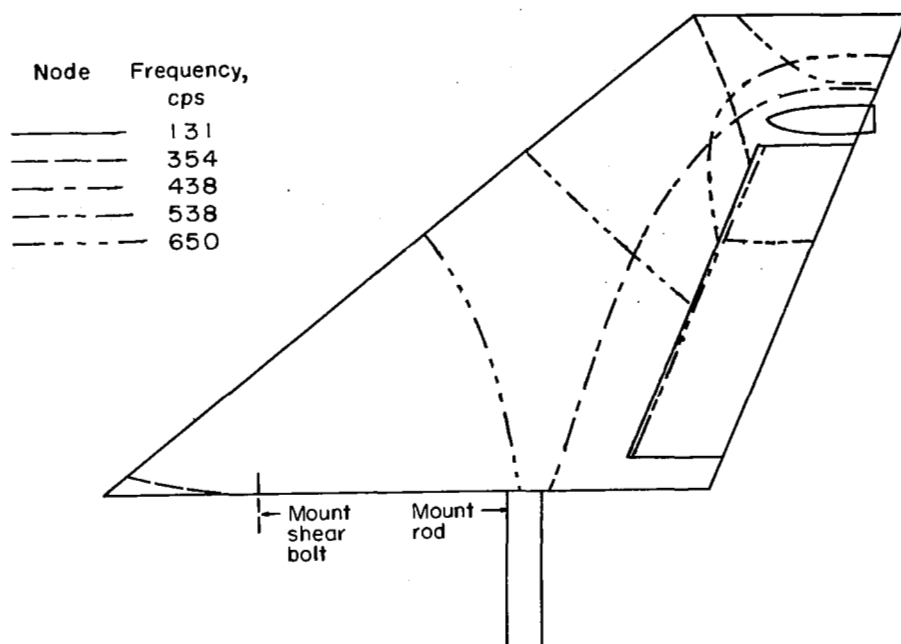


(e) Horizontal tail; $K = 2,260$ in-lb/radian; run 40.

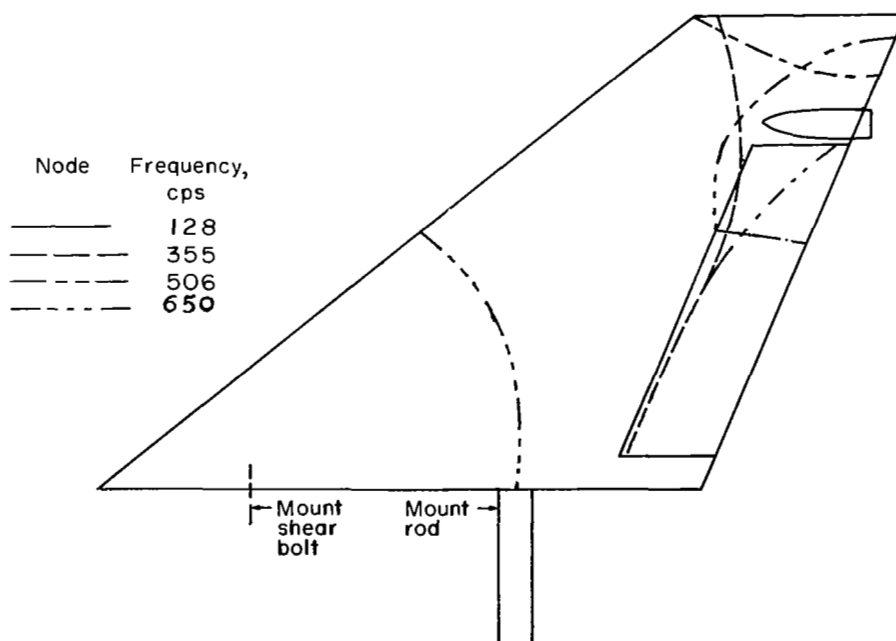


(f) Horizontal tail; $K = 1,174$ in-lb/radian; run 46.

Figure 6.- Continued.



(g) Vertical tail; $K_c = 136.5$ in-lb/radian; run 98.



(h) Vertical tail; $K_c = 52.3$ in-lb/radian; run 100.

Figure 6.- Concluded.

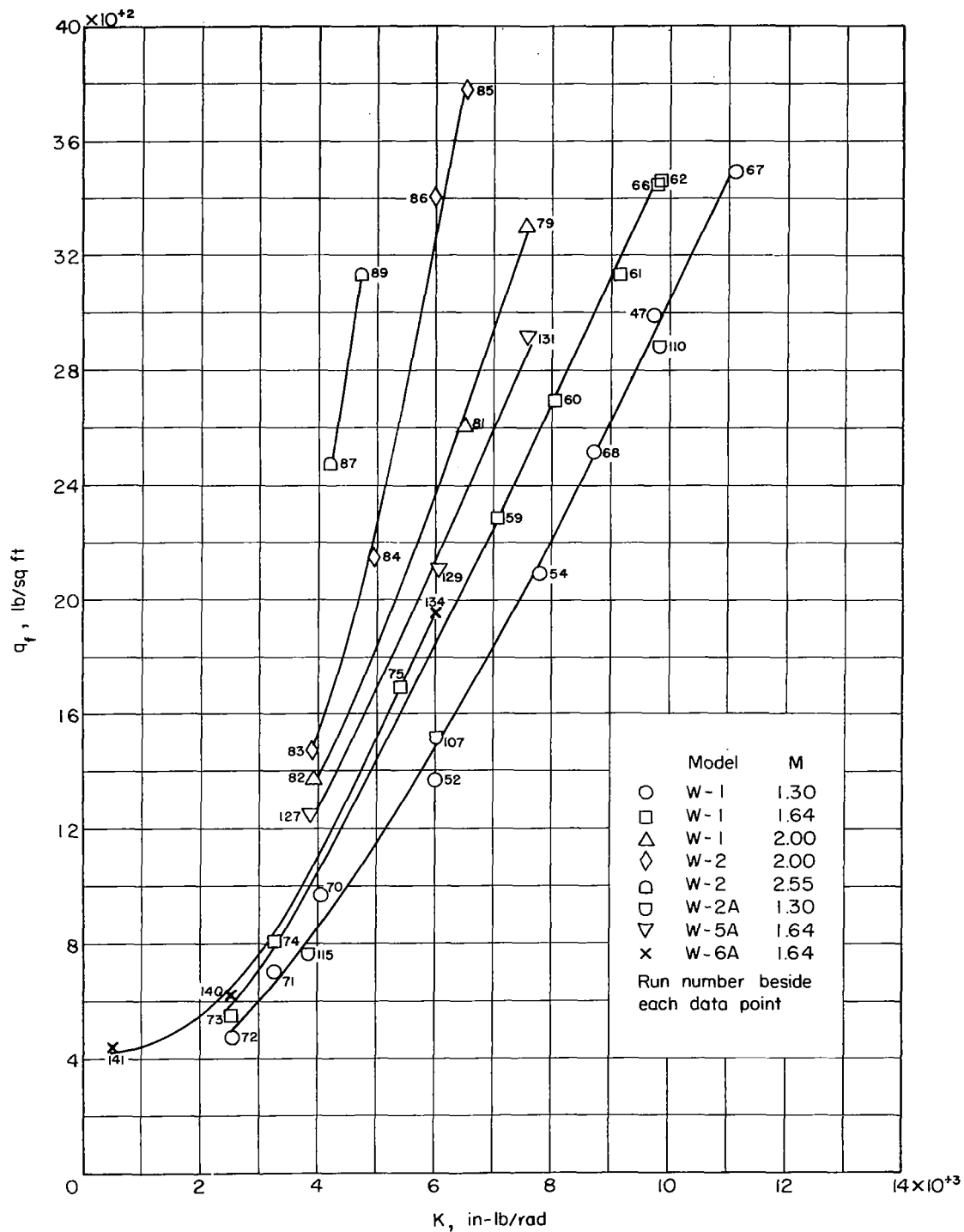
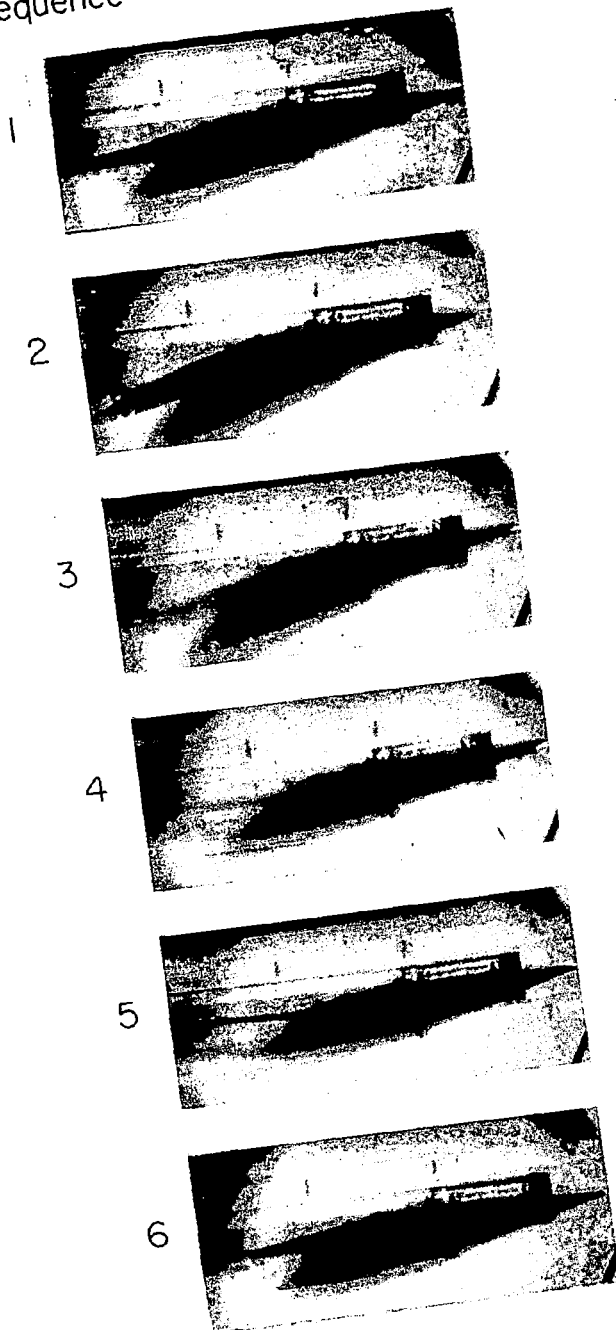


Figure 7.- Variation of dynamic pressure at flutter with pitch stiffness.

Sequence



Sequence

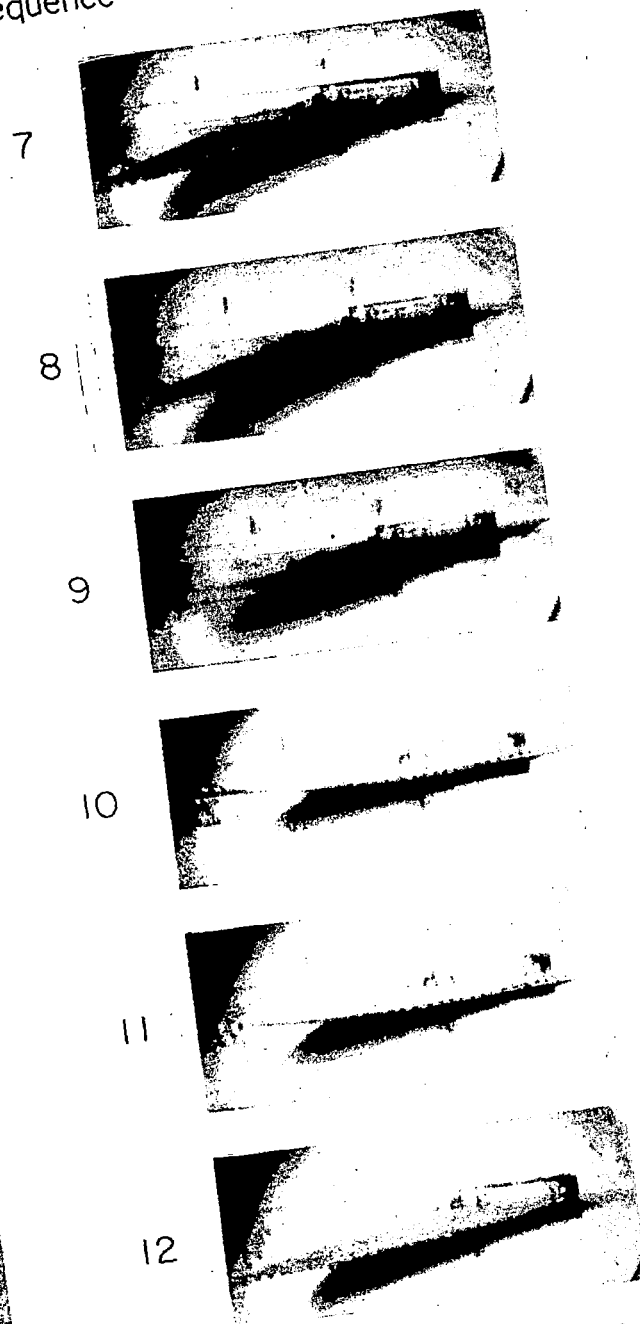
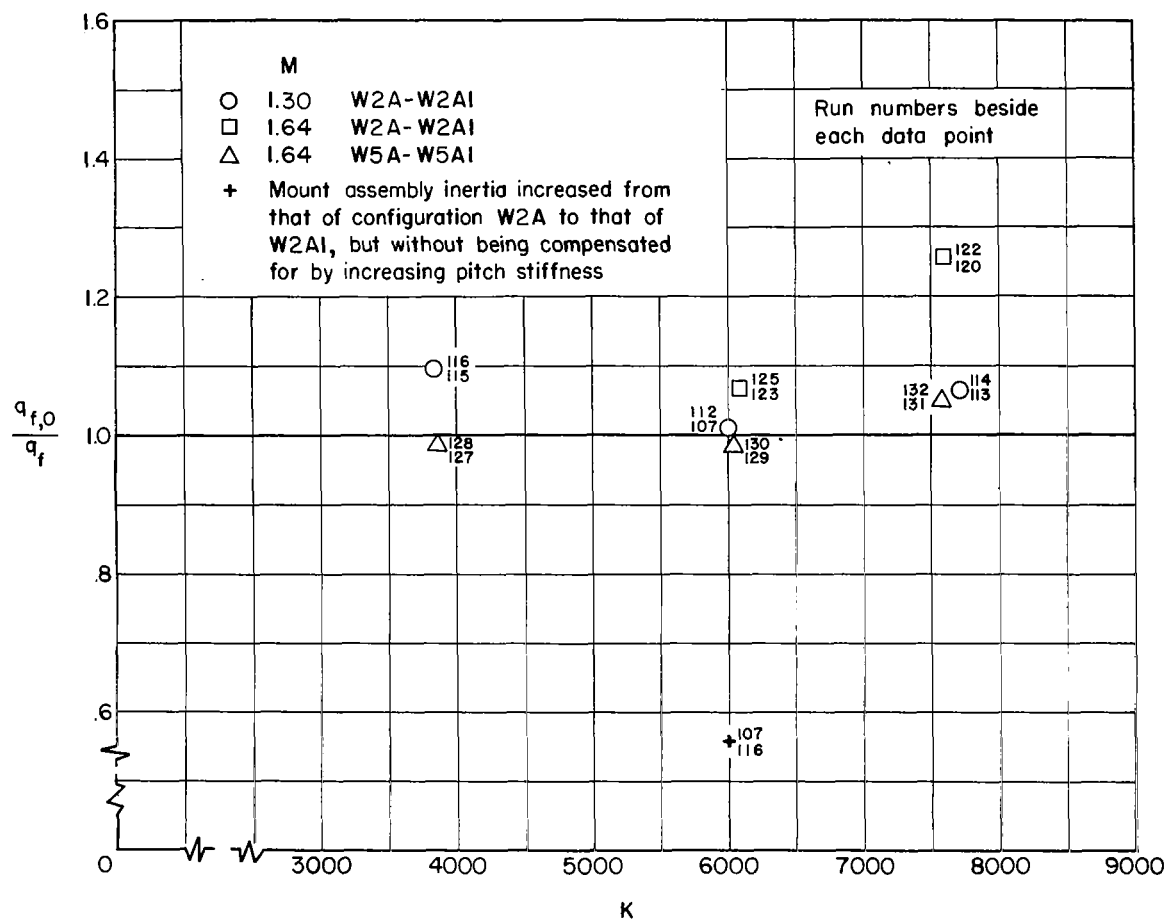


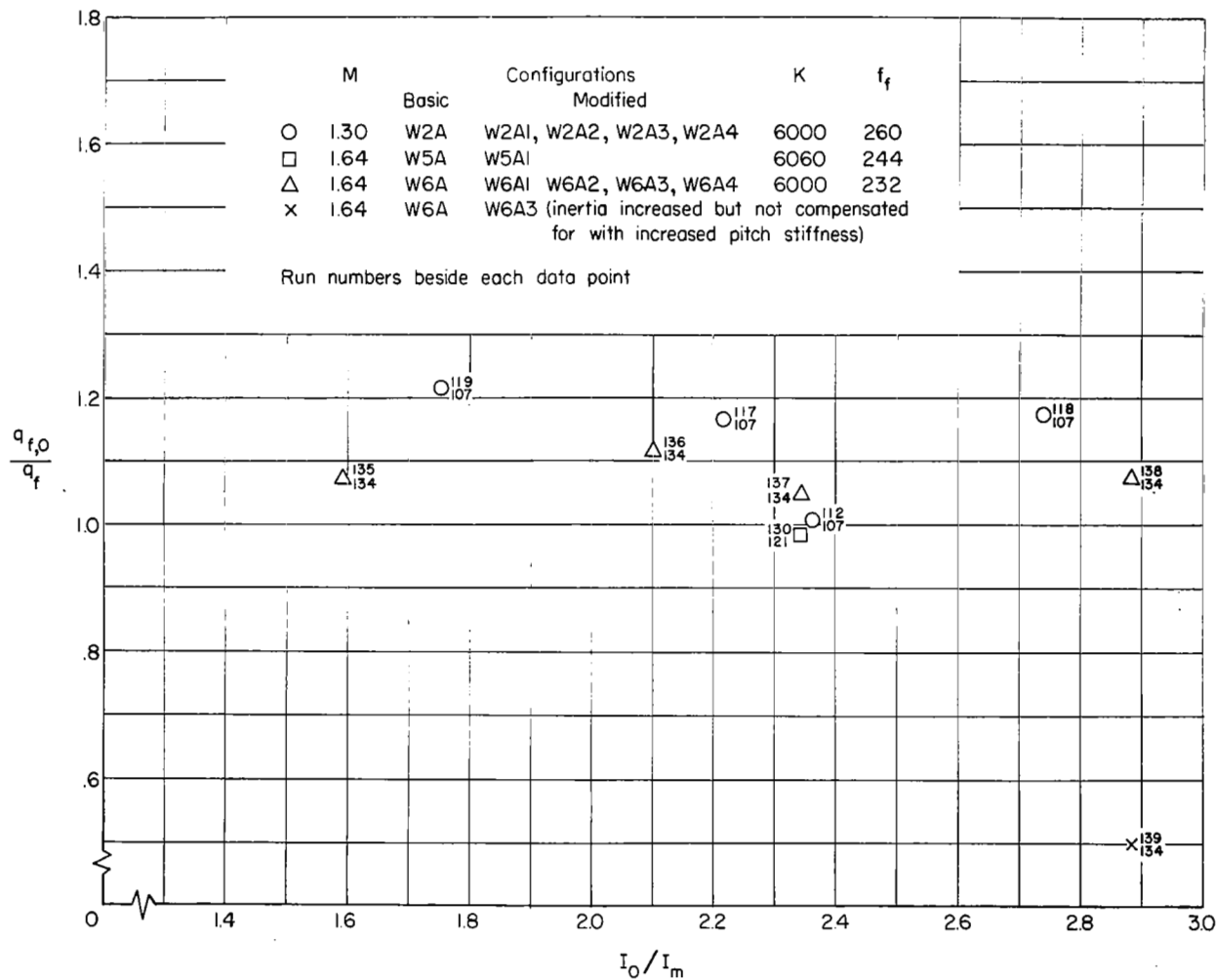
Figure 8.- Sequence from high-speed 16-millimeter motion picture illustrating wing flutter mode. Run 115; $f_f = 210$ cps.

L-58-2530



(a) $(I_0 - I_m)$ held constant while varying K with corresponding f_f .

Figure 9.- Effect on flutter dynamic pressure of changing mount assembly moment of inertia and compensating for the change by changing the pitch stiffness according to the relation $K_0 = K + 4\pi^2 f_f^2 (I_0 - I_m)$.



(b) K and corresponding f_f held constant while varying $(I_0 - I_m)$ by varying I_0 .

Figure 9.- Concluded.